Estimation of Forest Canopy Height Using Single Polarized TanDEM-X Across Different Forest Biophysical Characteristics in Temperate Forests

HAFTOM HAGOS GEBREMESKEL
June, 2022

SUPERVISORS:
dr. M. Schlund
drs.ing. M. Huesca Martinez

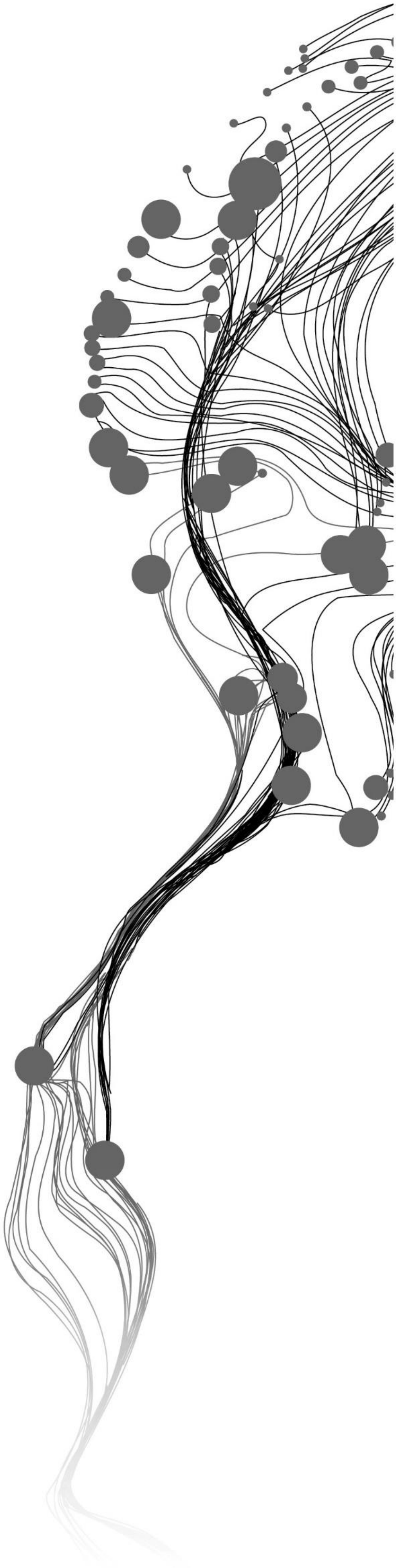

Estimation of Forest Canopy Height Using Single Polarized TanDEM-X Across Different Forest Biophysical Characteristics in Temperate Forests

HAFTOM HAGOS GEBREMESKEL
Enschede, The Netherlands, June, 2022

Thesis submitted to the Faculty of Geo-Information Science and Earth Observation of the University of Twente in partial fulfilment of the requirements for the degree of Master of Science in Geo-information Science and Earth Observation.
Specialization: Natural Resources Management

SUPERVISORS:
dr. M. Schlund
drs.ing. M. Huesca Martinez

THESIS ASSESSMENT BOARD:
dr., T. Wang (Chair)
dr. M. Schlund (Supervisor)
drs.ing. M. Huesca Martinez (Supervisor)
dr. Stefan Erasmi (External Examiner)
drs. R.G. Nijmeijer (Procedural advisor)

DISCLAIMER

ABSTRACT

Canopy height measurement is important to understand the forest's vertical structure and biomass quantification. In comparison to aerial-based, satellite-based canopy height estimation is useful in terms of covering large area and frequent measurements. TanDEM-X, a spaceborne active remote sensing, has been recently used to estimate canopy height. A simplified RVoG model was suggested to compute canopy height from TDX interferometric coherence. The model showed encouraging results in a well studied boreal forests and some temperate forests. Hence, the aim of this study is to further understand the simplified RVoG model (linear and sinc) on canopy height estimation of temperate forests considering forest type, slope class and canopy cover percentage. A single polarized TDX coherence data from five acquisitions with different height of ambiguity (HoA) was tested for the canopy height estimation. Two of the acquisitions were from October (with HoA of 35.2 m and 44.7 m) and three of acquisition were from January (with HoA of 41.3 m, 68.3 m, and 91.5 m). LiDAR point clouds were used to generate LiDAR canopy height and used it as reference. Root mean square error (RMSE), relative RMSE (RMSEr), coefficient of determination (R^2), absolute error (AE), and relative AE (AEr) were used to assess the accuracies. Mann Witney-U test and Kruskal-Wallis test were used to test difference between forest types and among slope classes, respectively. Linear regression was used to assess the impact of canopy cover percentage. A regression test was also held for one selected acquisition to analyse the impact of slope, and canopy cover estimation error. The results showed the RMSE and R^2 were different among acquisitions depending on the HoA and season of acquisition (leaf condition, precipitation, temperature). The RMSE ranged from 4.3 m to 5.7 m for the linear model and from 5.2 m to 16 m for the sinc model. The R^2 for both models were similar ranged from 0.14 to 0.48. The RMSEr and R^2 showed that coniferous forests had better estimation accuracies than broadleaved forests during the two October acquisitions, and one January acquisition that had high precipitation and temperature. In addition, for all acquisitions, the AEr showed that coniferous forest had significantly lower AEr than broadleaved forests. The RMSE and R^2 did not show a trend across slope classes, for all acquisitions. Whereas the AEr showed that, gentle slope had significantly lower AEr than steep slope for the two acquisitions with highest HoA. For similar acquisitions, the AEr significantly decreases with increasing canopy cover. The regression analysis showed that slope (coefficient = 0.24) and canopy cover percentage (coefficient = -0.54) significantly ($p<0.01$) explained 3% of the variation in absolute error for broad leaved forest. However, for the coniferous forests, only canopy cover percentage had significant ($p<0.05$) influence on absolute error, with an R^2 nearly to zero. Overall, canopy height estimation from single polarized TDX coherence gives moderate accuracy (RMSEr < 27%) across different biophysical characteristics of temperate forests. To obtain better accuracy for broadleaved forests, leaf season and weather conditions should be taken into consideration.

Key words: TanDEM-X, Coherence, Canopy height, Forest type, Temperate forests

ACKNOWLEDGEMENTS

I praise God for being a light to my path and unseen protection to my life.

I want to thank the OKP scholarship for sponsoring my study. My special appreciation goes to my supervisors, Michaele Schlund and Margarita Huesca Martinez, for their consistent guidance, support, and being friendly with me throughout my thesis work. You deserve ample gratitude. I would also like to thank Adiningrat Devara for your technical advice and for helping me provide some data. I want to thank the ITC student affairs staff for trying to help Tigrean students during the war on Tigray.

Finally, I thank my family for being with me spiritually and ITC friends and classmates, who contributed to my thesis in one way or other.

Dedicated to

The victims of Tigray Genocide and Tigrean martyrs who died fighting for survival

TABLE OF CONTENTS

LIST OF FIGURES

LIST OF TABLES

LIST OF APPENDICES

1. INTRODUCTION

Forests, which cover 31% of the earth's surface, are one of the main pools that dominates the dynamics of terrestrial carbon cycle and have an important share in the global carbon budget (FAO, 2020). Forests are a dominant carbon reservoir, constituting around 85% of the global above ground carbon (Schimel et al., 2001). Several studies have been conducted to study the benefit of forest to serve as a carbon sink and contributing to the global mitigation effort (Canadell and Raupach, 2008; Hoberg et al., 2016; Sedjo and Toman, 2001). These studies clarified the importance of measuring, quantifying, monitoring, and managing forests, as part of the global climate change mitigation. Besides, forest growth is dynamic and forest coverage can be decreased or increased over time due to natural and anthropogenic factors and this has implication on the total forest biomass. For example, temperate forests of Europe have shown an increment in forest growing stock of about 11.5% over the last 30 years, consequently increasing the amount of sequestered carbon (FAO, 2020). Such changes need to be monitored to understand the global carbon cycle and climate change.

Quantification of forest carbon can be done in destructive and un-destructive way. The destructive method requires cutting of trees, measuring the biomass in laboratory, and quantifying the carbon content as *ca*. 50% of the dry biomass (Liski et al., 2003). Though this method is accurate, it is environmental unfriendly and has limited practical applicability (Gibbs et al., 2007). Under the un-destructive methods, allometric equations are a well-known and widely used method to estimate biomass. It involves direct measurement of tree parameters such as tree height and diameter at breast height, subsequently, developing a regression equation for the forest biomass estimation (Chave et al., 2014). Besides to the biomass estimation, the measurement of tree height helps to understand the vertical structure of a forest which is essential for management, monitoring, and conservation purposes. Nevertheless, the *in-situ* measurement of the tree height is time consuming and labor intensive, especially when the forest covers a very large area (DeFries et al., 2007). In contrast, remote sensing measurements can estimate forest height which is advantageous in terms of time, labor, and areal coverage.

Remote sensors can be classified as passive and active sensors. Passive sensors have limited capability of retrieving vertical information, while data derived from active sensors allows to estimate vegetation structure (Zhang et al., 2017). Remotely sensed data to estimate canopy height accurately can be acquired from airborne platforms using Light Detection and Ranging (LiDAR). LiDAR is an active remote sensing technique which operates by sending laser beams from the sensor to gather ground and surface information as point clouds (Ferraz et al., 2016). The last and the first pulse returns in a certain grid cell forms digital terrain model (DTM) and digital surface model (DSM), respectively. A subtraction of DTM from DSM gives the canopy height model (CHM). In this sense, canopy height is the height of the highest point from ground in each specified grid. Forest height, as compared to tree height, is a little bit different concept, as it statistically describes tree heights over a certain area (Aulinger et al., 2005). It is the measurement of the trees forming the canopy height, which is an important concept from remote sensing point of view (Hajnsek et al., 2009). This way an accurate vertical information of forests can be retrieved. However, frequent measurements are not possible due to its high acquisition costs (Pirotti, 2011) and limited global availability (Lu et al., 2016). Canopy height can also be retrieved from images acquired from an Unmanned Aerial System (UAS) with high accuracy and low cost, whereas it is less applicable for large scale mapping (Kachamba et al., 2016).

Satellite sensors are widely used for large area mapping of forest vertical structures, like canopy height. Radar remote sensing, an active technique, is one of the alternatives for estimating and mapping canopy height. Radar sensors operate in the microwave spectrum where the wavelength ranged from 1 mm to 1 m, and they are widely known of their weather independence (ability to penetrate cloud) (Henderson et al., 1998). Synthetic Aperture Radar (SAR) sends and receives microwaves as backscatter which consists of amplitude and phase value of each resolution cell of an acquired image (Bamler and Hartl, 1998). In general, SAR data are mainly used for polarimetric and interferometric purposes. Polarimetric SAR (PolSAR) deals with the exploitation of the polarizations of the backscatter, where different combinations of transmission and receiving of horizontal (H) and vertical (V) waves are possible (horizontal transmission and horizontal receiving=HH, VV, HV, VH) (Cloude, 1998). It helps to understand the nature of the target object by retrieving its scattering properties (Cloude and Pettier, 1996). Interferometric SAR (InSAR) deals with the phase information of two SAR images to form interferometric coherence and acquire vertical information. Several studies have used PolInSAR, the combination of both PolSAR and InSAR, for accurate canopy height estimation (Fu et al., 2016; Kugler et al., 2014; Xie et al., 2017). PolInSAR acquisitions from airborne systems were used to acquire 3D information of forests (Hajnsek et al., 2009). A repeat pass acquisition like the L-band (ALOS-PalSAR) potentially provide the opportunity to retrieve the vertical information of a forest as it can fully or partially penetrate through the canopy (Ni et al., 2014). However, repeat-pass systems have the problem of temporal decorrelation associated with a time gap between the two acquisitions (Kugler et al., 2014). Temporal decorrelation happens when the scattering properties of an object is changed, in between two acquisitions, induced by different factors such as wind (Bamler and Hartl, 1998). The change in scattering properties of an object degrades the quality of interferometric coherence which is usually formed as the phase function of the two acquisitions. Consequently, the decrease in coherence highly affects the height estimation accuracy. The problems associated with temporal decorrelation can be significantly minimized by a single-pass acquisition of two spatially separated antennas, in which one example of an operational spaceborne system is known as the TanDEM-X (hereafter referred as TDX) mission (Martone et al., 2012).

A commonly used method to estimate height from TDX is an inversion of Random Volume over Ground (RVoG) model (Kugler et al., 2014). To obtain canopy height from this model inversion, it requires the interferometric coherence, ground topography, ground-to-volume ratio and wave extinction in the volume scattering (Kugler et al., 2015). The inversion of RVoG model is normally possible in the presence of full polarimetric data (Khati et al., 2017). However, the TDX mission is mainly available in single polarization (HH) in its standard acquisition mode (Gomez et al., 2021). Having the single polarized data, the RVoG inversion can be used if the ground topography information is obtained from external data sources (Chen et al., 2019). It can also be used to directly subtract the LiDAR Digital Terrain Model (DTM) from the TDX height (phase center height) (Sadeghi et al., 2016, 2014). However, the global availability of LiDAR data is limited. Recently some studies suggested to use The Global Ecosystem Dynamics Investigation (GEDI) LiDAR data to obtain ground information (Chen et al., 2021; Qi et al., 2019; Qi and Dubayah, 2017). However, the GEDI data is limited to the range between 51.6 N and 51.6 S latitudes, and the data are sampled footprints and not available as a wall-to-wall data ("Home Page - GEDI," n.d.). Hence, a canopy height estimation without the support of external DTM would have wider applicability and can also be used at large scale.

With single polarized mode and no external ground topographic information, simplification of the RVoG model is proposed to make the model invertible (Kugler et al., 2014). Canopy height has been estimated using this simplified model in temperate forest (Schlund et al., 2019), Mediterranean forest (Gomez et al., 2021) and boreal forest (Olesk et al., 2016). The performance of TDX to estimate canopy height depends on different factors attributed to TDX acquisition parameters (Sadeghi et al., 2017) and biophysical characteristics of the forest (Kugler et al., 2014). TDX acquisition parameters like effective baseline (distance between the two satellites), incidence angle and height of ambiguity affects the accuracy of the height estimation (Gomez et al., 2021; Sadeghi et al., 2017). Canopy cover density (Olesk et al., 2015b), forest type (Chen et al., 2019; Gomez et al., 2021; Olesk et al., 2015b), forest vertical structure (Erasmi et al., 2019; Olesk et al., 2015b), phenology (leaf-on or leaf-off) (Olesk et al., 2015b; Sadeghi et al., 2017; Schlund et al., 2019) and slope of the underlying topography (Gomez et al., 2021; Schlund et al., 2019), are among the biophysical factors affecting the accuracy of TDX height estimation. Studies conducted in Canadian boreal forest and Estonian hemi-boreal forest revealed that TDX height estimation has higher accuracy in coniferous forests than in broadleaved forest during leaf-on season (Chen et al., 2019; Olesk et al., 2015b). This is justified as the broadleaved trees hinder the X-band penetration during the leaf-on season, resulting in a lack of volume scattering information from the lower canopy. This results in poor estimation compared to the leaf-off season (Kugler et al., 2014; Olesk et al., 2015b). The other reason might be due the fact that X-band has a different penetration capability in different forest types (Kugler et al., 2014; Olesk et al., 2015b). The canopy cover density also affects potentially the X-band penetration, determining the accuracy of TDX height estimation which is studied in boreal/hemi-boreal forests (Olesk et al., 2015b; Persson and Fransson, 2016; Sadeghi et al., 2017) and Mediterranean forest (Gomez et al., 2021). However, the effect of forest types and canopy cover density on accuracy of single polarized TDX height estimation is not well studied in temperate forests. Hence the aim of this study is to estimate the canopy height using single polarized TDX in temperate forest and assessing its accuracy considering different stratification of forest type, canopy cover density and slope.

2. OBJECTIVES AND RESEARCH QUESTIONS

2.1. General objective

- The general objective of this study was to estimate canopy height using TDX coherence in broadleaved and coniferous forest of temperate forests

2.2. Specific objectives

- To estimate canopy height using TDX with linear and sinc models
- To compare the accuracy of TDX canopy height estimation between broadleaved and coniferous forests
- To compare the accuracy of TDX canopy height estimation across different slope classes (Flat, gentle, and steep slopes)
- To analyze the impact of canopy cover percentage on TDX canopy height estimation accuracy

2.3. Research questions

- What is the accuracy of linear and sinc models in TDX canopy height estimation?
- Is the accuracy of TDX canopy height estimation similar between broadleaved and coniferous forests?
- How does the accuracy of TDX canopy height estimation vary across different slope classes?
- Does the variation in canopy cover percentage significantly affect the accuracy of TDX canopy height estimation?

3. STUDY AREA AND DATASETS

3.1. Study area

The study area was in the Gelderland province, the Netherlands, which covered parts of the Hoge veluwe and Veluwezoom national parks. The study area is geographically located between 5°49'10"E to 6°1'47" N and 51°59'1" N to 52°8'28" N and it has an area of 216 km² (Figure 1). A weather station is located in Deelen, Gelderland, inside the study area, where the long-term average annual precipitation (1991 to 2021) is 871 mm. January is the coldest month with a mean temperature of 2.9°C and May is the warmest month having a mean temperature of 18.1°C (KNMI - Daily Values Precipitation Stations, n.d.). The area is mostly dominated by coniferous species of *Pinus sylvestris, Larix decidua*, *Pseudotsuga menziesii* and broadleaved trees of *Sorbus aucuparia, Quercus robur* and *Quercus petraea* (Hein, 2011; Kuiters et al., 2006, 2005). In the Hoge veluwe national park, *Pinus sylvestris* dominated coniferous trees cover 27% and broadleaved trees cover 10% of the park. In the Veluwezoom national park *Pinus sylvestris* is dominant covering 42% of the park and broadleaved trees cover 23% of the park (Te Linde et al., 2012).

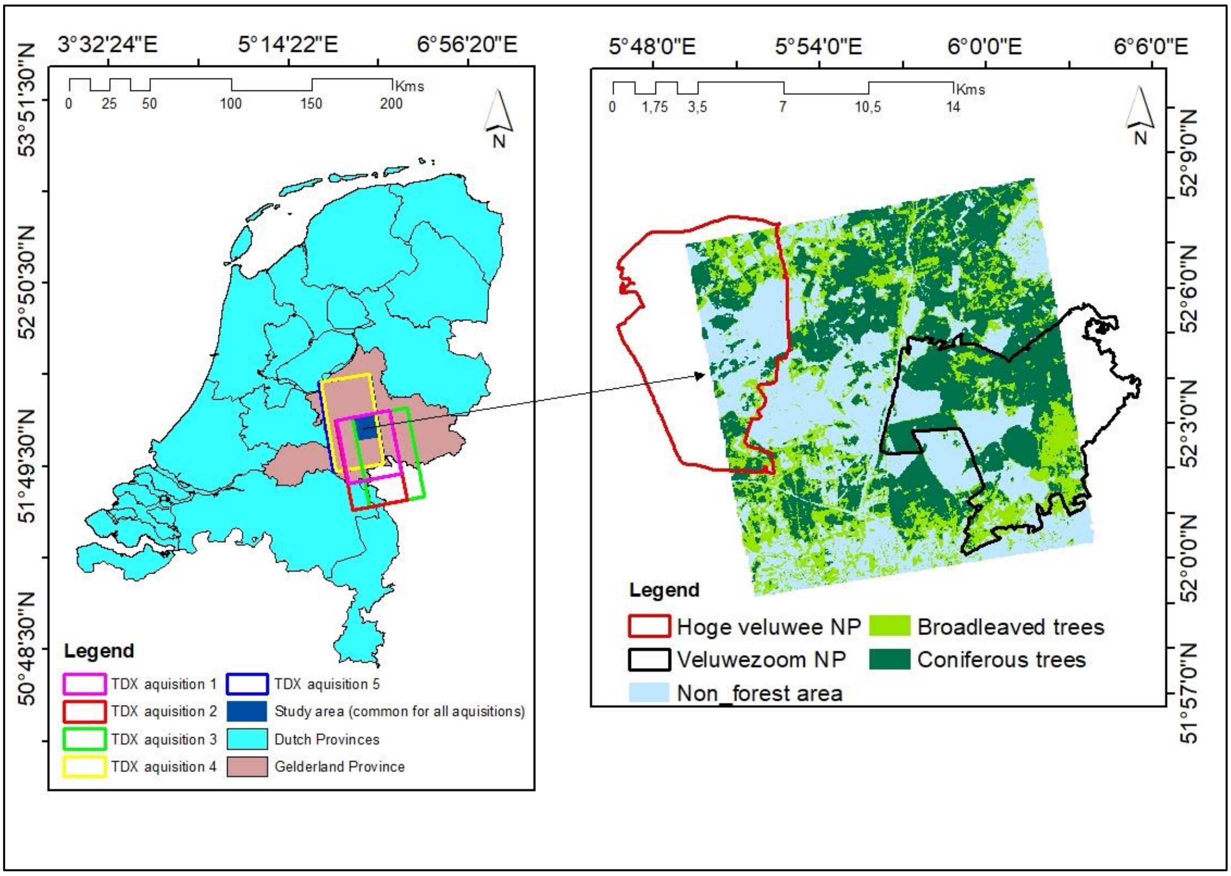

Figure 1 Map of the study are and the forest types

3.2. Datasets

3.2.1. TDX data

Single-pass interferometric data was acquired from twin satellites of the TDX mission flying in close formation, where they acquire X-band data with high-resolution and potentially multi-polarized. These two almost identical satellites perform a simultaneous single-pass acquisition, which avoids the effect of temporal decorrelation (Abdullahi et al., 2016). The data are acquired in the bistatic mode, in which one of the sensors transmit waves and both receive the backscattered wave. The available TDX data contains five images from the years of 2011 and 2012 (Table 1) (The order of acquisitions in figure 1 are the same order as in Table 1). All the images have single polarization of Horizontal-Horizontal mode (HH) and were acquired in ascending orbit. The spatial coverage of all the images did not fully overlap. Hence, a common area corresponding to the five images was selected as study area for the ease of comparison (Figure 1). The acquisitions have different incidence angles, effective baselines, and heights of ambiguity (HoA) and were acquired during the months of October and January. Effective baseline is the distance between two satellites and incidence angle is the angle between the line of sight and the incident radiation from the illuminated object (Richards, 2009) in which both determine the HoA (Zink et al., 2014). HoA is "*the vertical distance between two points that yield the same interferometric phase value*" (Krieger et al., 2010). For each TDX acquisition, the mean temperature and sum precipitation data for the date of acquisition and one day before were obtained from KNMI website.

Table 1 Summary of the TDX dataset

Date	Incidence angle (̊)	Effective baseline (m)	|HoA| (m)	Kz (rad/m)	Pixel resolution (m) (Range × Azimuth)	Pixel spacing (m) (Range × Azimuth)
October-31-2012	37.05	170.92	35.2	0.18	2.9 × 3.3	1.36 × 2.06
January-04-2011	46.25	199.14	41.3	0.15	2.4 × 3.3	1.36 × 2.17
October-12-2011	36.18	129.77	44.7	0.14	3 × 3.3	1.36 × 2.03
January-19-2012	36.18	85.56	68.3	0.09	3 × 3.3	1.36 × 1.91
January-24-2012	34.59	89.84	91.5	0.07	2.4 × 3.3	1.36 × 2.17

3.2.2. LiDAR data

LiDAR technique is well known and widely used in vegetation studies for its high performance in terms of geolocation precision and height measurement accuracy (Popescu and Wynne, 2004). As a result, a LiDAR system was frequently used as a reference for satellite-based canopy height estimations (Guliaev et al., 2021; Olesk et al., 2015b; Persson et al., 2017; Schlund et al., 2019). A LiDAR system produces point cloud in which the points stored 3D information of a target area (Douillard et al., 2011). The height file for Netherlands (AHN2) was acquired from 2007 to 2012, between the months of December and March every year ("Kwaliteitsbeschrijving | AHN," n.d.). The LiDAR measurement year varies depending on the area. For the study area, AHN2 was collected in 2010. The acquisition season was more or less similar with the TDX acquisition season which was acquired in January and October. The acquisition year of AHN2 had one to two year difference with the acquisition year of all TDX data. The files are available in https://esrinl-content.maps.arcgis.com/apps/Embed/index.html?appid=a3dfa5a818174aa787392e461c80f781 in the form of point clouds and grids. The point cloud data, with X, Y, Z coordinates, contained two separate files of filtered ground and non-ground level returns. The data had a density of 6 to 10 points/m^2 with a height accuracy of ≤ 20 cm and planimetric accuracy of ≤ 23 cm ("Kwaliteitsbeschrijving | AHN," n.d.).

3.2.3. Forest map data

A map of forest types for the year 2012 was downloaded from Copernicus website (https://land.copernicus.eu/pan-european/high-resolution-layers/forests/dominant-leaf-type/status-maps/2012). The map consisted of forest types (in the source described as 'dominant leaf type') namely coniferous and broadleaved forests for whole Europe extracted from multitemporal satellite data and classified using Support Vector Machine (European Environment Agency, 2021). Forest type map of the study area is shown in figure 1. This map was chosen considering its high spatial resolution (20 meter), high overall thematic accuracy (>90%) and its data availability for the required year (2012) to be consistent with the TDX and LiDAR acquisitions ("Copernicus Land Monitoring Service User Manual Consortium Partners," n.d.). The map was clipped to the extent of the study area. Coniferous trees cover 80.3 km² and broadleaved trees covers 49.6 m² constituting 37% and 23% of the study area, respectively.

3.3. Methodology

3.3.1. Methodological Flow chart

The general methodology followed in this study is illustrated in Figure 2. The acquisition parameters mentioned in the chart refers to baseline, incidence angle, range distance and HoA.

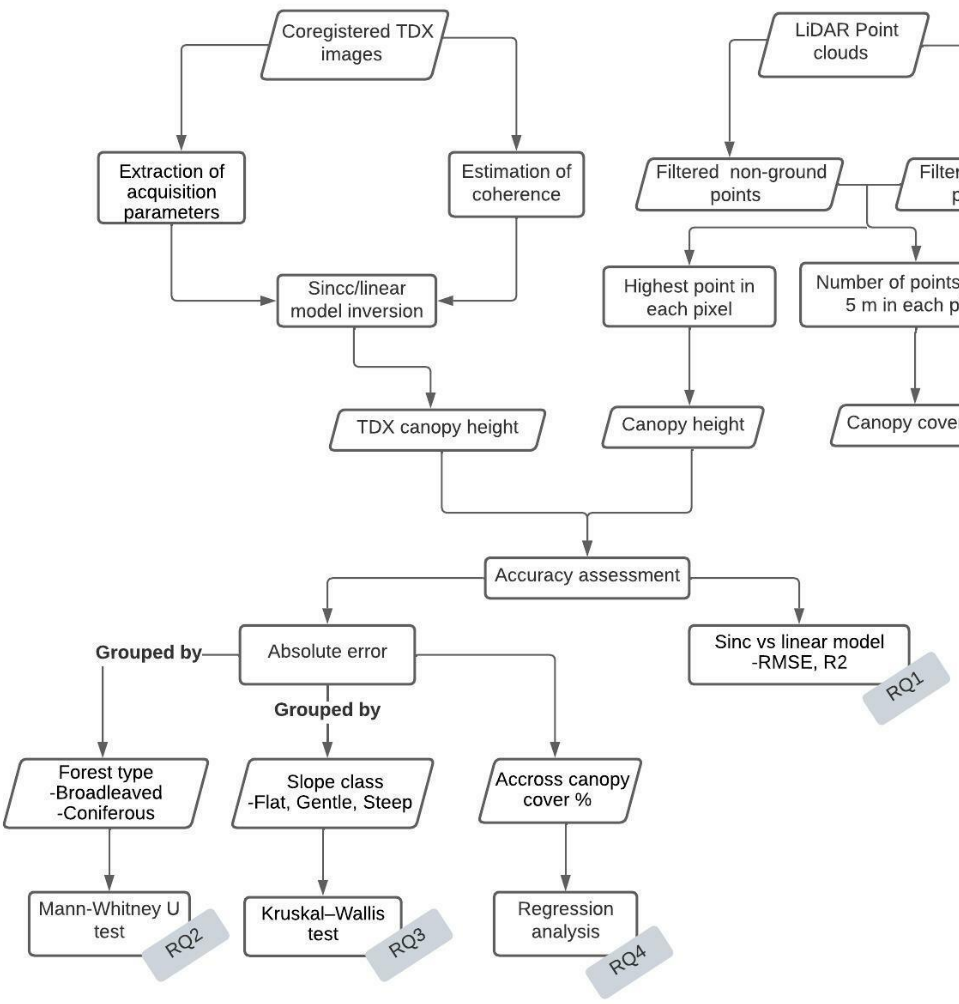

Figure 2 A flow chart showing the overall methodology

3.3.2. Estimation of LiDAR canopy height and canopy cover

The FUSION software was used to generate canopy height model (CHM) from the filtered ground and non ground point clouds. The ground point clouds were grided to 20 m resolution to form the ground level DTM. From the ground level points, the highest return within each 20 m cell was taken to produce the CHM as used by (Chen et al., 2015; Coops et al., 2007; Lovell et al., 2003) to represent h_{100}. h_{100} is a standard forest height parameter which takes the average of 100 tall trees per hectare to represent forest height of an area (Hajnsek et al., 2009). For lidar canopy height, the approximate h_{100} can be obtained by considering the maximum point in a 10 by 10 meter cell (Kugler et al., 2014; Aulinger et al., 2005; Hajnsek eta al., 2009). The CHM used in this study was not the exact mimic of the h_{100} due to its low spatial resolution (20 m) used as compared to other studies (10 m).

In addition to the CHM, the LiDAR points were used to map the slope and canopy cover density of the study area. The slope percentage was derived from the LiDAR DTM. Canopy cover is one of the forestry metrics used to describe forests' vertical and horizontal structure (Zhang et al., 2017). The canopy cover is a numerical value which is expressed in terms of percentage. Canopy cover percentage was computed as ratio between points above 5 meter and all LiDAR returns in a 20 by 20-meter grid cell.

3.3.3. Estimation of TDX canopy height

Simplified RVoG model

The Random volume over ground (RVoG) model is a two-layer scattering model that enables canopy height inversion from the InSAR coherence under certain assumptions (Kugler et al., 2014). It assumes a uniform forest canopy layer (volume scattering) over an impenetrable ground layer (Olesk et al., 2016). RVoG model inversion needs independent measurements of polarization dependent ground phase, ground-to-volume ratio and volume coherence. This requires a polarimetric data and the equation for volume coherence can be described as

$$\gamma_{vol} = \exp(ik_z z_0)\frac{\gamma\text{v}+\text{m}}{1+\text{m}} \qquad (1)$$

where γ_{vol} means interferometric coherence, k_z means vertical wave number, Z_o means reference (ground) height, γ_v means volume only decorrelation and m means ground-to-volume ratio.

γ_v can be calculated as

$$\gamma_v = \exp\,(ik_z z_0)\frac{\int_0^{hc}\exp\,(2\sigma z/\cos\theta)\,\exp\,(ik_z z_0)dz}{\int_0^{hc}\exp\,(2\sigma z/\cos\theta)dz} \qquad (2)$$

Where hc is the canopy height and σ extinction coefficient

k_z can be calculated using Baseline (Bn), wavelength (λ), incidence angel (θ) and Range distance (R).

$$k_z = \frac{4\pi\text{Bn}}{\lambda\text{R}\sin\theta} \qquad (3)$$

In a single polarized acquisition, the number of observable parameters is less than that of unknown parameters, making the model inversion in (1) impossible. The unknown parameters here are m, σ and Z_o. To make the inversion possible certain assumptions needed to be applied (Olesk et al., 2016). One of the assumptions is to consider the ground has no contribution in the coherence (assuming the X-band does not reach the ground). Hence, the volume-to-ground ratio were assumed to be zero (Hajnsek et al., 2009). The other assumption was to keep extinction coefficient constant over the forest as zero (Kugler et al., 2014). By doing this, the model remained with two known (coherence and vertical wave number) and one unknown variable (canopy height). The HoA can be computed from the vertical wave number (k_z) as (Olesk et al., 2016).

$$\mathrm{HoA} = \frac{2\pi}{\mathrm{Kz}} \quad (4)$$

Finally, the RVoG model could be simplified to a sinc model as

$$|\gamma_{vol}\mathrm{sinc}| = \mathrm{sinc}\left(\pi * \frac{hc}{\mathrm{HoA}}\right) \quad (5)$$

Where γ_{vol} means the interferometric coherence, *hc* means the canopy height, and HoA means height of ambiguity

Inversion of sinc function in (5) requires a look up table. Hence, for the ease of calculation, an approximation to (5) can be calculated using (6) (Chen et al., 2016). A linear model (7) was also used to compute canopy height where the simplified RVoG model is assumed to work best when the maximum canopy height does not exceed the HoA (Olesk et al., 2016; Schlund et al., 2019).

$$hc = \mathrm{HoA}^{\times}|1 - \frac{2}{\pi}{}^{\times}\sin^{-1}({\gamma_{vol}}^{0.8})| \quad (6)$$

$$hc = \mathrm{HoA}^{\times}|1 - \gamma_{vol}| \quad (7)$$

Where γ_{vol} means the interferometric coherence and *hc* means the canopy height

The coherence was estimated using the master and slave images. This was followed by multilooking of 20 m spatial resolution to align with the resolution of available forest type map. Georeferencing and terrain correction was done, and an elliptical incidence angle image was produced besides the coherence image. Both coherence and elliptical incidence angle images were used for further processing.

Range time for each corner and center of the image was extracted from the xml file of TDX data. Range distance was then calculated as in (8). From this five data points (four center and one corner) a raster layer of range distance was created by interpolation. Baseline information for each acquisition was also obtained from the xml file. The Kz and HoA were computed using (3) and (4), respectively. Finally, the TDX canopy height (*hc*) was estimated using a sinc and linear model as seen in (6) and (7), respectively.

$$\text{Range distance} = \frac{\text{Range time}*\text{speed of light}}{2} \quad (8)$$

3.4. Comparison of accuracies

For the comparison, around 10% of the pixels (Schlund et al., 2019) were extracted in a stratified random sampling method assuring representative pixels are accounted across the forest type, canopy cover and all slope classes. All areas with canopy height less than 5 meter were excluded from the analysis as they are considered as non forest area, according to FAO definition. The accuracy assessment was done using three accuracy metrics namely; root mean square error (RMSE), coefficient of determination (R^2), and absolute error (AE). The RMSE and R^2 were used to compare the estimation accuracies between models, acquisitions, forest types, slope classes, and canopy cover. Whereas the AE was used to test significance difference between different classes of forest and slope. To ensure comparability of accuracies across different canopy height values, the relative RMSE (RMSEr (%)) and relative AE (AEr (%)) were used. The RMSE, AE and their relative terms were computed as seen in (9) to (12).

$$RMSE = \frac{\sqrt{\sum_{i=1}^{n}(CHM_i - hc_i)^2}}{n} \quad (9)$$

Where i is individual observation, CHM_i is the LiDAR canopy height, hc_i is the TDX canopy height and n is the number of observations

$$\mathrm{RMSEr_c}\ (\%) = \frac{RMSE_c}{CHMc_c} \times 100 \qquad (10)$$

Where c refers to one class of forest type or slope class, $\mathrm{RMSEr_c}$ (%) is the relative RMSE of group c, $\mathrm{RMSE_c}$ is the RMSE of group c, and $\overline{CHM_c}$ is the mean CHM of group c

$$AE_i = |CHM_i - hc_i| \qquad (11)$$

$$AEr_i\ (\%) = \frac{AE_i}{CHM_\mathrm{i}} \times 100 \qquad (12)$$

Where i is individual observation representing each sample point, AE_i is the absolute error of ith observation, AEr_i (%) is the relative absolute error of i^{th} observation, hc_i is the TDX canopy height of i^{th} observation and, CHM_i is the CHM of i^{th} observation

3.4.1. Comparison of height estimations across forest types

To compare the variation in accuracy of TDX height estimation over the two forest types, the estimation was divided in to broadleaved and coniferous. As the coniferous forest covered large area, the number of sample pixels was higher (12809 pixels) than broadleaved forest (7179 pixels). Hence, the number of samples for coniferous was kept to 7179 in a random selection to make a balanced sample. Thereafter, the absolute error (11) was computed for each observation. Normality distribution of the errors was checked to select appropriate significance test. For both forest types, the errors were not normally distributed. As a result, a non-parametric test for two groups (Mann-Whitney U test) was used to test the group difference at p-value of 0.05. The test was made on the relative absolute error (12), to mitigate any impacts that may arose from the height variation between the two forest types.

3.4.2. Comparison of height estimations across slope classes

A Food and Agricultural Organization (FAO) slope classification scheme were used to classify the study area into different slope classes (Table 2) (Iaaich et al., 2016). This enabled to make a comparison of the height estimations across different slope classes. The study area was dominated with a flat to moderate slope (Table 2). To some extent there were also steep slopes. The number of samples for each slope class were heavily unbalanced. The samples in each class were balanced to 1621 pixels. The absolute errors for each class were not normally distributed. Other processes were similar to section (3.4.1) except the Kruskal Walis test held which is relevant for more than two groups.

Table 2 Slope classes of the study areas (FAO)

	Area coverage in km² (The % in bracket are column-wise)			
Slope class (%)	Coniferous	Broadleaved	Non-forest	Total
0-3	31.3 (39%)	18.8 (38%)	47.8 (55.7%)	97.9
3-12	42.2 (52.6%)	23.9 (48.2%)	33.0 (38.5%)	99.1
12-20	4.8 (6%)	4.5 (9.1%)	3.3 (3.8%)	12.6
>20	1.9 (2.4%)	2.4 (4.8%)	1.7 (2%)	6.0
Total	80.3 (100%)	49.6 (100%)	85.8 (100%)	215.7

3.4.3. Effect of canopy cover on height estimation

Forest structure is the vertical and horizontal arrangement of forest structural parameters (McElhinny et al., 2005) which can be explained in different metrics such as height based, canopy density based and canopy volume metrics (Zhang et al., 2017). In this study, the parameter considered for forest structure was the canopy cover percentage. A regression model was used to investigate how the variation in canopy cover affects the TDX height estimation accuracy. The canopy cover was used as independent variable and the absolute estimation error, as dependent variable. In addition, the regression was again done after the canopy cover percentage was grouped into every 5% interval.

Furthermore, it is important to assess the contribution of the slope and canopy cover to the height estimation error. Since the independent variables had different range of values, they were standardized to make their effects comparable. This was done by subtracting a mean from each value and dividing by the standard deviation (Miuigan et al., 1988). Then after, a regression was developed between the estimation error (dependent variable) and the slope and canopy cover percentage separately for both forest types. The significance of the independent variable coefficients was determined with their respective p-values.

4. RESULTS

4.1. Canopy height estimation

4.1.1. LiDAR canopy height model

The forest canopy height of the study area ranged from 5.0 m to 43.6 m (Figure 3). The average canopy height of the study area was 21.1 m with a standard deviation of 5.2 m. About 72% of the forest had a canopy height between 15.0 m to 25.0 m and 18% of the forest had a canopy height above 25.0 m. The rest falls between 5.0 m to 10.0 m canopy height. The broadleaved and coniferous forests had a mean canopy height of 22.0 m and 21.6 m. The mean canopy height in the flat, gentle, and steep slope was 19.8 m, 21.1 and 22.3 m, respectively.

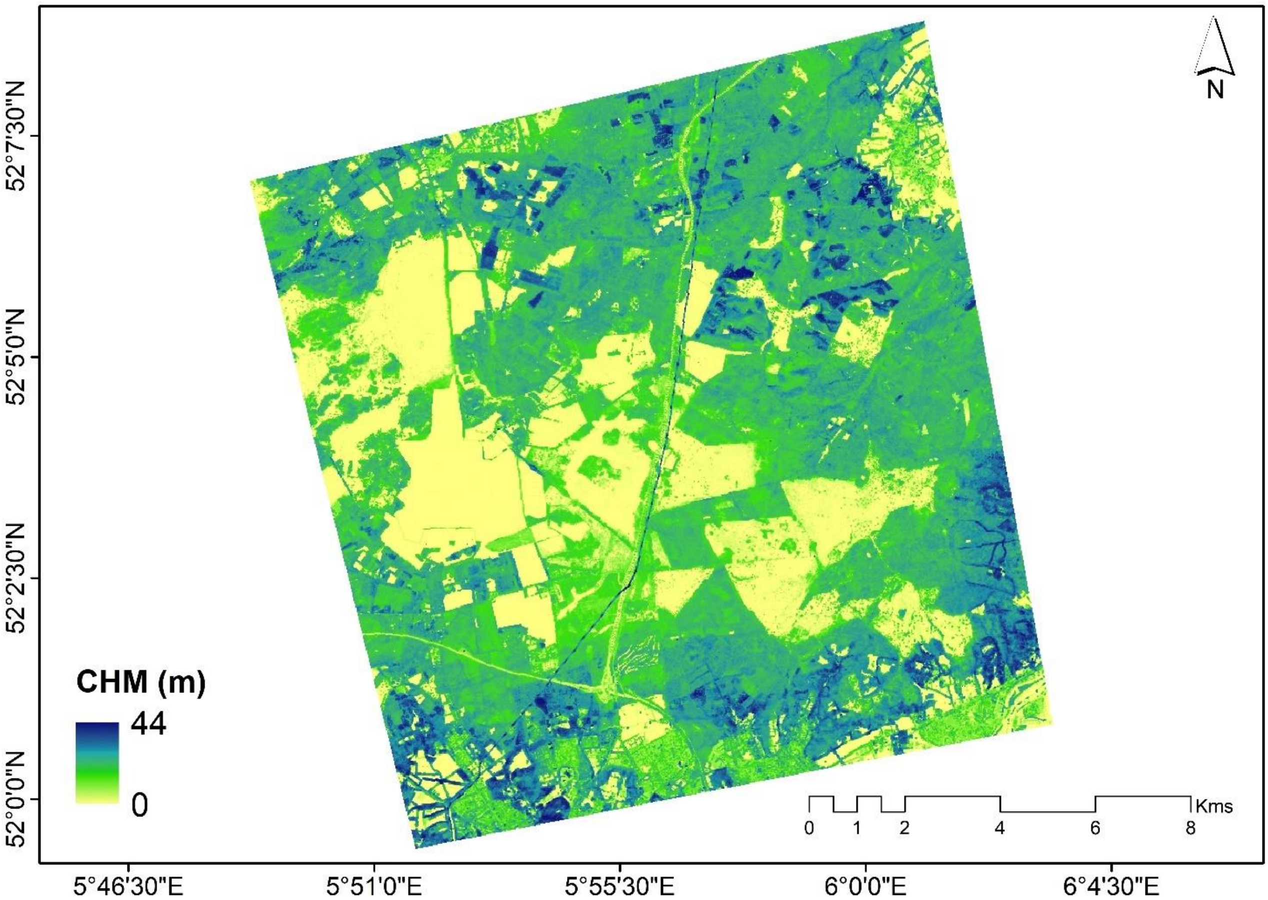

Figure 3 LiDAR canopy height map of the study area

4.1.2. Coherence estimation of TDX

The coherence descriptive statistics of all the acquisition which are ordered in ascending order of the HoA are summarized in Table 3. The coherence of the five datasets was different based on their respective HoA and other factors (Table 3). The January 24 acquisition with highest HoA (91.5 m) had a high average coherence and low standard deviation. It also had high kurtosis and high negative skewness showing that a large amount of data concentrated in a small range of high coherence values. This was somehow similar to January 19 acquisition of the other high HoA (68.3 m). In comparison to the above two acquisitions, the other three acquisitions had lower mean coherence (<0.58), higher standard deviation (>0.10), lower kurtosis (<0.18), and lower skewness (Table 3).

Table 3 Descriptive statistics of coherence

					Coherence					
Acquisition date	Acquisition id (Acq. id)	HoA (m)	Temperature (ºC)	Precipitation (mm)	Min	Max	Mean	Standard deviation	Skewness	Kurtosis
October-31-2012	October 31	35.2 m	7.05	1.4	0.09	0.82	0.41	0.11	0.20	-0.41
January-04-2011	January 04	41.3 m	-0.75	0	0.14	0.90	0.51	0.12	-0.03	-0.39
October-12-2011	October 12	44.7 m	12.6	27.6	0.11	0.89	0.58	0.11	-0.51	0.18
January-19-2012	January 19	68.3 m	3.6	14.7	0.14	0.93	0.65	0.09	-1.05	1.83
January-24-2012	January 24	91.5 m	2.85	1.7	0.38	0.95	0.76	0.06	-1.18	2.53

In all acquisitions, the estimated coherence had negative relationship with the CHM normalized by HoA (Fig 3). In other words, the coherence decreased as the ratio of canopy height to HoA increased. In the first three acquisitions (October 31, January 04 and, October 12), when the CHM/HoA was above 0.6 there was no a clear trend. In the last two acquisitions (January 19 and January 24), the CHM/HoA was less than 0.6 and the coherence increased as the ratio decreased. In the first three acquisitions (October 31, January 04 and, October 12), most of the data points were extended from the linear to sinc lines (Figure 4). In the last two acquisitions (January 19 and January 24) where the HoA was high, the observations were far below the sinc model whereas well fitted with the linear model.

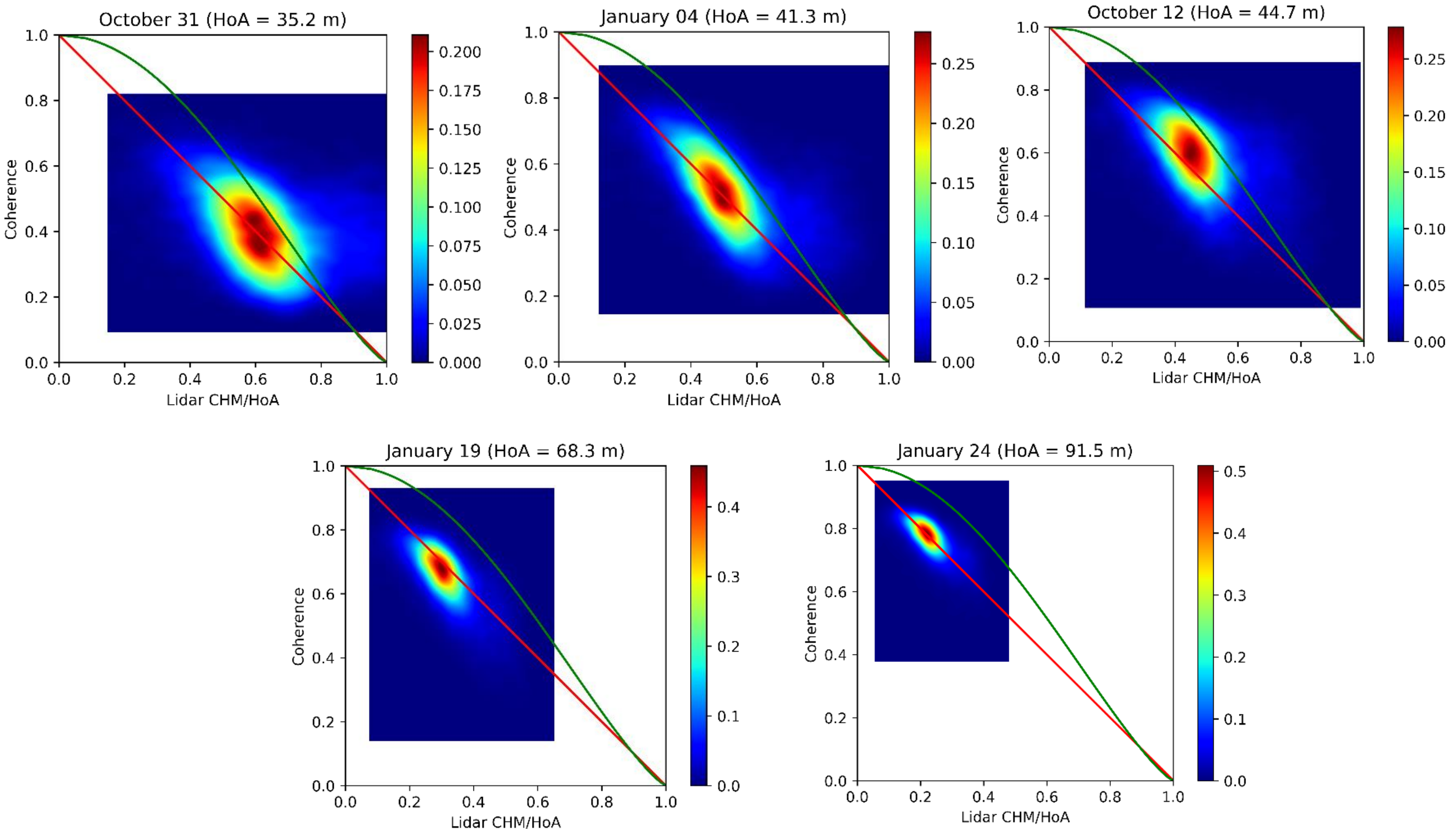

Figure 4 Color density scatter plot of CHM/HoA versus estimated coherence of different acquisitions (the red and green line showed the linear and sinc models, respectively)

4.1.3. Canopy height estimation with TDX

For the linear model, the estimated canopy height ranged from 4.1 m (January 04) to 56.8 m (January 19). The October 12 and January 19 acquisitions had the lowest (18.6 m) and highest average canopy height (23.6 m), respectively (Table 4). For the first three acquisitions with lower HoA (October 31, October 12, and January 04), the average canopy height was less than the average CHM. The average canopy height of the other two acquisitions with high HoA (January 19 and January 24) were above the average CHM (Table 4). In comparison with the CHM, the RMSE for all acquisitions ranged from 4.3 m (January 24) to 5.7 m (October 12) and R^2 ranged from 0.14 (October 31) to 0.47 (January 19) (Table 4). In general, the two October acquisitions had higher RMSE (>5.3 m) and lower R^2 (<0.25) in comparison with the RMSE (<5.2 m) and R^2 (>0.38) of January acquisitions.

Table 4 Summary of descriptive statistics and accuracy metrics (linear and sinc models)

	Acq. id	HoA	Height (m) Min	Max	Mean	Standard deviation	RMSE	R^2
CHM			5.0	43.6	21.1	5.2		
Linear	October 31	35.2	6.2	30.0	20.0	3.8	5.3	0.14
	January 04	41.3	4.1	35.6	20.2	4.8	4.5	0.38
	October 12	44.7	4.9	38.8	18.6	4.9	5.7	0.25
	January 19	68.3	4.6	56.8	23.6	6.1	5.2	0.47
	January 24	91.5	4.3	56.5	21.5	5.3	4.3	0.44
Sinc	October 31	35.2	12.0	29.9	22.8	2.7	5.2	0.14
	January 04	41.3	10.5	35.9	24.7	3.5	5.5	0.38
	October 12	44.7	12.0	38.8	24.4	3.7	5.7	0.25
	January 19	68.3	14.2	57.4	33.4	4.7	12.9	0.48
	January 24	91.5	15.9	63.2	36.5	4.7	16	0.44

For the sinc model, the estimated canopy height ranged from the minimum of 10.5 m (January 04 acquisition) to the maximum of 63.2 m (January 24 acquisition). The lowest and highest average canopy height was observed for the acquisitions of October 31 (22.8 m) and January 24 (36.5 m), respectively (Table 4). The lowest RMSE was observed for October 31 acquisition (4.3 m) and the highest was for January 24 acquisition (16 m). For all the acquisitions, the average canopy height was higher than the average CHM. For the sinc model of January 24 acquisition, as seen in Figure 5, the higher density points were below the 1:1 graph indicating the overestimation of the sinc model. The overestimation of sinc model was observed in other acquisitions as well (Appendix 3). The RMSE of the linear and sinc models were similar for the October 31, October 12, and January 04 acquisitions. However, for the January 19 and January 24 acquisitions the RMSE of the sinc model was higher than that of the linear model (Table 4). The R^2 for all acquisitions was similar with the linear model. As the linear model performed better than the sinc model, further analyses were focused on the linear models.

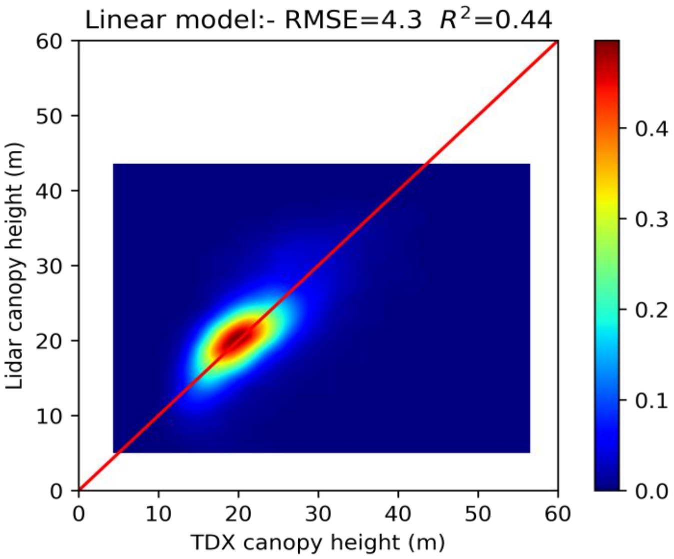

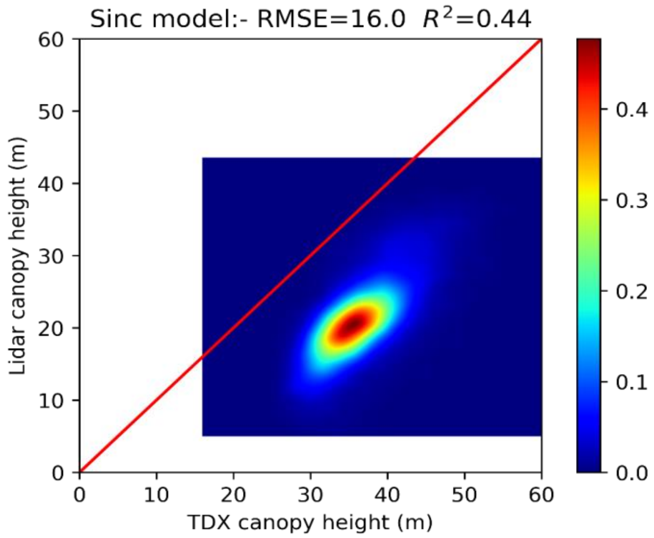

Figure 5 Scatterplot of CHM and TDX estimated height for linear and sinc models of January 24 acquisition with the red line indicating 1:1 relation (scatterplots for all acquisitions are in Appendix 2 and 3).

Overall, better performance was observed for the linear model of January 24 acquisition (the highest HoA) with lowest RMSE of 4.3 m and second highest R^2 of 0.44. The absolute error map of the January 24 acquisition revealed that most of the forest areas had absolute estimation errors less than 6 m (Figure 6). The absolute error map for other acquisitions is shown in Appendix 1.

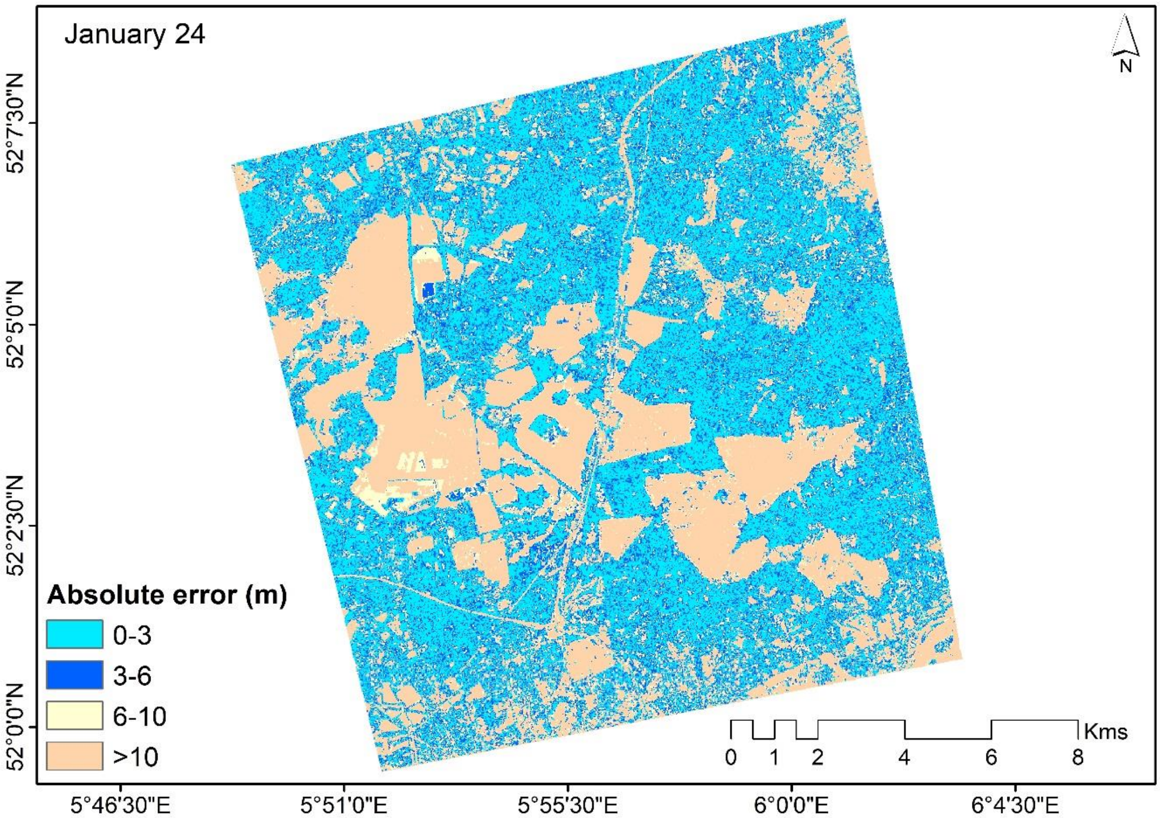

Figure 6 Absolute difference between CHM and linear TDX height of January 24 acquisition

4.2. TDX canopy height estimation of Broadleaved and coniferous forests

For the broadleaved forest, the R^2 generally improved with increasing HoA (Table 5). Apart from the HoA, the season had an impact in the R^2. For the two acquisitions in October, the R^2 tended to be low (0.09 and 0.16) (Table 5). For the three acquisitions made in January, the R^2 was relatively high (> 0.40) as compared to the October acquisitions. The RMSE in broadleaved forest ranged from 4.8 m to 6.8 m where the highest RMSE was recorded for the October acquisitions with RMSE of 6.3 m and 6.8 m (Table 5). For the January acquisitions the RMSE was less than 6.1 m. The HoA did not clearly show an impact on the RMSE.

Table 5 Comparison of accuracy metrics of different acquisition across forest types

		Broadleaved			Coniferous		
Acq. id	HoA (m)	RMSE (m)	RMSEr (%)	R^2	RMSE (m)	RMSEr (%)	R^2
October 31	35.2	6.3	28.7	0.09	4.7	22.8	0.18
January 04	41.3	4.8	21.9	0.40	4.4	21.4	0.35
October 12	44.7	6.8	31.0	0.16	4.9	23.8	0.32
January 19	68.3	6.1	27.8	0.50	4.6	22.3	0.44
January 24	91.5	4.8	21.9	0.47	4.0	19.4	0.40

The RMSE for all acquisitions of coniferous forests ranged from 4.0 m to 4.9 m. Though the RMSE values were similar, there was a general decreasing trend with increasing the HoA. Moreover, the R^2 showed increasing trend with increasing HoA. The season of acquisition did not have an impact on the R^2. For instance, the acquisitions on January 04 and October 12 were from different seasons but had similar HoA (41.3 m and 44.7 m), they showed similar R^2 (0.35 and 0.32) and RMSE (4.4 m and 4.9 m) (Table 4).

Comparing the RMSEr of both forest types, the impact of season of acquisition on the RMSE was observed for the broadleaved forests. The RMSEr difference between the broadleaved and coniferous forest for the October 31 and October 12 was 5.9% and 7.2% respectively, which was higher than that of the RMSEr difference in the January 04 (0.5%) and January 24 (2.5%). There was an exception for the January 19 acquisition where the RMSEr difference of between the broadleaved and coniferous was 5.5 %. Apart from the RMSE, the relative mean of absolute errors (MAEr) for coniferous forest was significantly lower than that of the broadleaved forest for all acquisitions (Table 6).

Table 6 A Mann-Whitney U test of group difference between broadleaved and coniferous forests

Acq. id	Forest type	MAEr (%)	Standard deviation	P-value
	Broadleaved	21.9	22.6	
October 31	Coniferous	17.0	15.6	<0.0001
	Broadleaved	17.2	18.4	
January 04	Coniferous	15.5	13.8	<0.001
	Broadleaved	24.0	23.2	
October 12	Coniferous	18.6	15.0	<0.0001
	Broadleaved	24.0	29.3	
January 19	Coniferous	18.5	18.9	<0.0001
	Broadleaved	18.6	27.1	
January 24	Coniferous	15.3	17.3	<0.001

Number of samples for each forest type is 7179

4.3. TDX height estimation across slope classes

There was a slight difference in the RMSEr across slope classes for all acquisitions. The minimum RMSEr was 16.7% for the October 12 acquisition in gentle slopes and the maximum was 25.7% for January 19 acquisition in steep slopes (Table 7). The highest RMSEr difference of 3.9% was observed between gentle and steep slope in the acquisition of January 19 (Table 7). Regarding R^2, there was no substantial difference across slope classes for all acquisitions. The largest difference was for October 12 acquisition where the R^2 increased by 0.06 from gentle slope to steep slope.

Table 7 Summary of accuracy metrics across slope classes

		Flat slope		Gentle slope		Steep slope	
Acq. id	HoA (m)	RMSEr (%)	R^2	RMSEr (%)	R^2	RMSEr (%)	R^2
October 31	35.2	18.0	0.16	16.7	0.17	17.1	0.12
January 04	41.3	17.5	0.32	17.2	0.32	17.1	0.28
October 12	44.7	22.2	0.15	21.1	0.18	22.1	0.12
January 19	68.3	22.0	0.22	21.8	0.22	25.7	0.25
January 24	91.5	18.0	0.19	17.5	0.20	19.9	0.19

Number of samples for each slope class was 1621

The MAEr was not significantly different between slope classes for the acquisitions of October 31, January 04, and October 12 where the HoA was small (Table 8). For the acquisition of January 19, the MAEr of steep slope was significantly higher compared to the two other classes and there was no significant difference between the flat and gentle slope. For the acquisition January 24 a significant variation was observed between gentle and steep slope (Table 8).

Table 8 Kruskal-Wallis significance test of MAEr across slope classes

Acq. id	HoA (m)	Slope class	MAEr (%)	Standard deviation	Sig
October 31	35.2	Flat	14.6	11.4	0.208
		Gentle	13.6	10.5	
		Steep	13.9	10.7	
January 04	41.3	Flat	13.8	10.9	0.657
		Gentle	13.9	10.6	
		Steep	13.8	10.9	
October 12	44.7	Flat	17.9	12.7	0.185
		Gentle	17.2	12.4	
		Steep	17.9	12.7	
January 19	68.3	Flat	17.4[a]	14.7	<0.001
		Gentle	17.1[a]	14.6	
		Steep	19.6[b]	17.0	
January 24	91.5	Flat	13.5[ab]	12.5	<0.05
		Gentle	13.0[a]	12.3	
		Steep	14.4[b]	14.7	

Number of samples for each slope class was 1621. *Means with different letter show sig. variation

4.4. Impact of canopy cover on TDX height estimation

The canopy cover of the study area ranged from 0 to 99.9 % (Appendix 6). Most parts of the study area had a canopy cover between 25% and 75%, which accounts for 91%. 7% of the area had a canopy cover less than 25% and the rest 2% had canopy cover above 75%. For all acquisitions, there was a relationship between the height estimation accuracy and the canopy cover. As the canopy cover increased, the estimation accuracy decreased for all acquisitions but with very small R^2 ($R^2<=0.05$). However, when the canopy cover was grouped in every 5% interval (<5%, 5%-10%, 10%-15% and so on), a significant relationship was found with high R^2 values, for the two acquisitions having high HoA. The MAEr significantly decreased with increasing canopy cover having an R^2 of 0.72 and 0.46 for January 19 and January 24 acquisitions, respectively (Figure 7). For the acquisitions with HoA less than 45 m, the MAEr did not show an increasing or decreasing trend with increasing canopy cover.

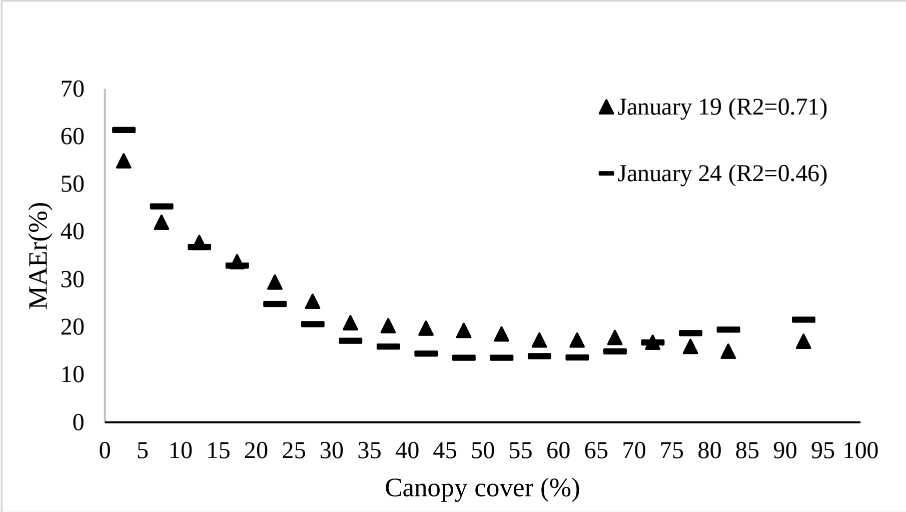

Figure 7 Relationship between MAEr and grouped canopy cover (%) for acquisitions of January 19 and January 24

4.5. Contribution of canopy cover and slope to estimation error

The slope and canopy cover were brought together in an attempt to make a regression against the absolute estimation error separately for broadleaved and coniferous forest. This was solely done to the January 24 acquisition. Both, slopes and canopy cover, significantly (P-value <0.01) explained only 3% of the variation in absolute error for broadleaved forests (Table 9). The sign of the coefficients indicated that with increasing slope and decreasing canopy cover, the absolute error increased for broadleaved forests. For this forest type, the coefficient was higher for canopy cover than the slope.

For coniferous forests, the R^2 was very low but the influence of canopy cover on absolute error was observed. However, slope did not explain the variation in absolute error for coniferous forests. The coefficients of canopy cover suggested that the impact of canopy cover was less for coniferous forests as compared to broadleaved forests

Table 9 Regression table of dependent (absolute error) with standardized slope and canopy cover

	Broadleaved (R^2 = 0.031)		Coniferous (R^2 = 0.001)	
	Coefficient	p value	Coefficient	p value
Intercept	3.20	<.001	2.90	<0.001
Standardized slope	0.24	<.001	0.01	=0.668
Standardized canopy cover	-0.54	<.001	-0.069	<0.05

5. DISCUSSIONS

5.1. TDX canopy height estimation

This study attempted to understand a linear and sinc models in estimating canopy height from TDX coherence values under different biophysical characteristics like forest type, slope, and canopy cover. The sinc model in all acquisitions overestimated the canopy height compared to the linear model. The overestimation was especially higher (>12 m) for the acquisitions with higher HoA (January 19 and January 24 acquisitions). Conceptually, Chen et al. (2016), elucidated that a sinc model should always underestimate the height; however, their test in Canadian boreal forest showed otherwise. This might be related to some problems of coherence correction procedures (Chen et al., 2016), which was not applied in this study. A study in temperate forests also found a sinc model to generally overestimate the height; especially when the HoA is above 60 m, the RMSE goes above 12 m (Schlund et al., 2019). For the current study, as the linear model had better accuracies than sinc, further discussions were made based on the results of linear model.

The RMSE and R^2 ranged from 4.3 m to 5.7 m and from 0.16 to 0.47 for all acquisitions. Similar study in temperate forest found comparable results with RMSE of 6.2 m to 13.5 m and R^2 of 0.08 to 0.62 (Schlund et al., 2019) even for higher spatial resolution (12 m) as compared to this study. TDX canopy height estimation accuracy varied with the HoA, the acquisition season, temperature, precipitation, and other factors. All the January acquisitions had lower RMSE and higher R^2 than the October acquisitions. The highest RMSE difference was between January 24 and October 12 which was 1.4 m. The fact that both acquisitions had different HoA and season of acquisition (attributed to leaf and weather conditions) might have contributed to the difference in the RMSE. The impact of season of acquisition can be seen by comparing October 12 (HoA = 41.3 m) and January 04 (HoA = 44.7 m) acquisitions. Despite having comparable HoA, the January 04 acquisitions performed better in terms of RMSE and R^2 (Table 4). The January 04 acquisition was a leaf-off season with lower temperature and precipitation than the October 12 acquisition (Table 1), which could be the possible reason for the variation in the RMSE. Previous studies also observed that season of acquisition affected accuracy of TDX canopy height estimation (Olesk et al., 2015b; Schlund et al., 2019).

The HoA did not have linear relationship with canopy height estimation error. This might be due to the variation in weather variables (temperature and precipitation), which potentially decreased the impact of HoA. For example, considering the January acquisitions (HoA of 41.3 m, 68.3 m and 91.5 m), the ones with lowest and highest HoA had lower temperature and precipitation than the middle one (Table 1), which possibly could undermine the impact of HoA. Similar results were found in temperate and boreal forests where cold and dry weather was associated with better estimation accuracy (Schlund et al., 2019). Variations in weather variables change the vegetation's dielectric properties, which affects its scattering behaviors. High precipitation and temperature increase the dielectric constant of the vegetation, leading to increased attenuation of microwaves by the canopy, which may result in height overestimation (Solberg et al., 2015). During wet conditions, coherence is influenced by the water in vegetation in addition to other characteristics of the forest (canopy height, cover, structure and so on) (Olesk et al., 2015b). The presence of precipitation increases volume decorrelation and decreases coherence, subsequently high estimation errors (Olesk et al., 2015b; Sadeghi et al., 2017). Figure 8 also illustrated that RMSE increased with increasing of temperature and precipitation. While it is quite understandable why the RMSE for January 19 acquisition (HoA=68.3 m) was high, it remained challenging to explain why it had highest R^2.

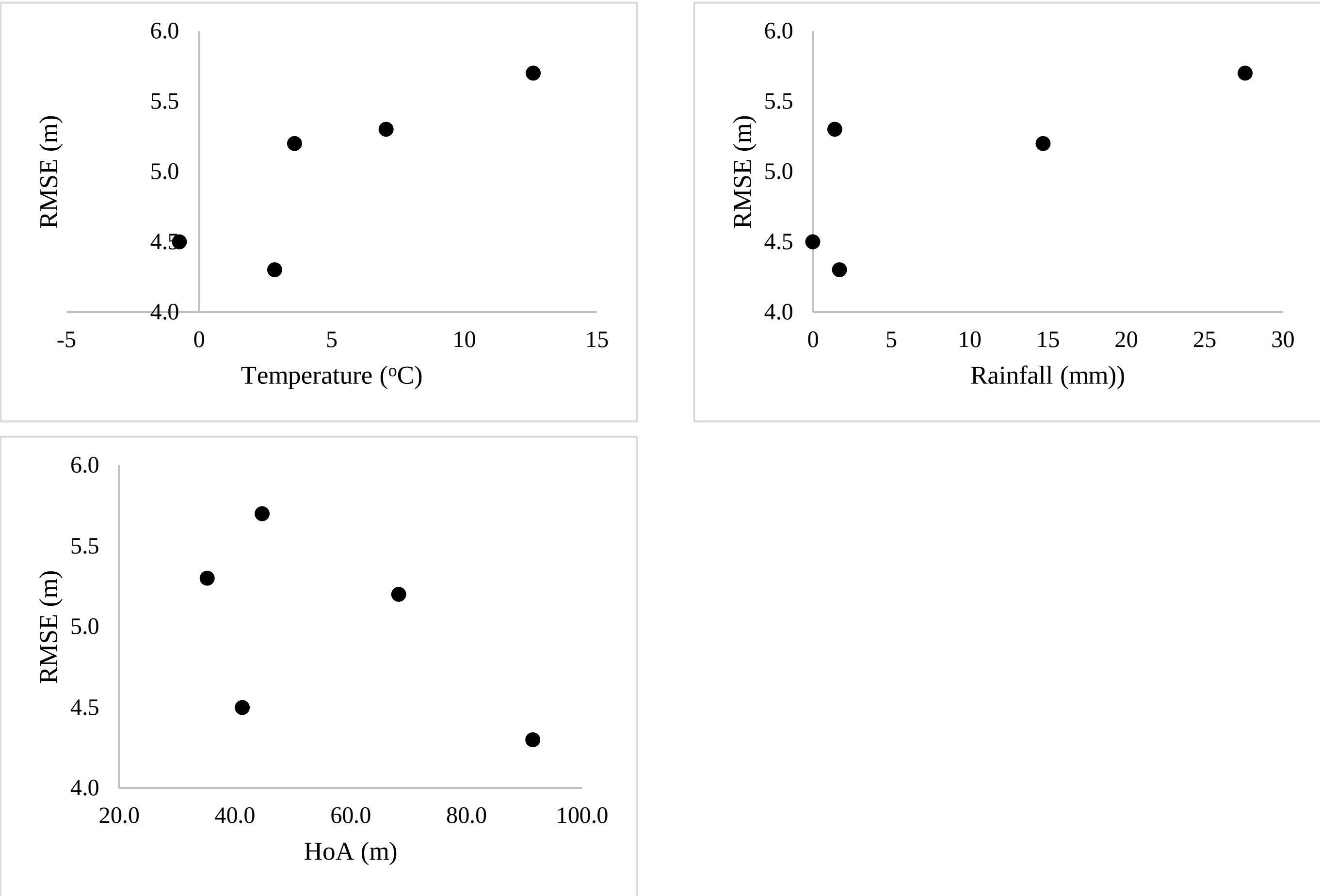

Figure 8 Relationship of RMSE with temperature, precipitation and HoA

Comparing January 04 and January 24 acquisitions which had contrasting HoA but similar temperature and precipitation, the RMSE was lower for the large HoA than the small HoA. This indicated that HoA had an impact on accuracy, but it also depends on the condition on the ground. Moreover, our study observed that the relationship between HoA and estimation accuracy depended on the canopy height (Appendix 7). The two acquisitions with highest HoA (68.3 m and 91.5 m) had the smaller RMSE than others when the canopy height was above 30 m. For the same acquisitions, the RMSE was higher (RMSE >=10 m) when the canopy height was less than 10 m. This is because of the high difference between the canopy height and HoA. The interferometric system becomes less sensitive as the canopy height gets much lower than the HoA, consequently, the estimation accuracy reduces (Gomez, 2021). Chen et al. (2016) suggested small HoA for better canopy height estimation of small canopies. Similarly in this study, one of the acquisitions with small HoA (41.3 m) had better RMSE (6.3 m) than other acquisitions when the canopy height is less than 10 m (Appendix 7). In addition, the acquisition with lowest HoA (35.2 m) had the highest RMSE (13.1 m) when the canopy height was above 30 m. This is in line with the study of Khati et al. (2017), which found the estimation error increases with increasing canopy height for small HoA and vice versa for large HoA. Olesk et al. (2016) also explained that the linear model does not work well when the canopy height is closer to the HoA. Another study by Chen et al. (2016) proposed a HoA of two to four times of the canopy height for better estimation accuracy. In other words, this is a canopy height ranging from 25% to 50% of the HoA. Also, for this study, depending on the HoA, better accuracy (RMSE <4.5 m) was found within the canopy height ranged from 20% to 65% of the HoA. In this study it is understood that different acquisitions had their best accuracy over different canopy height classes (Appendix 7). As a result, a combination of acquisitions with different HoA (multi-baseline) has been recommended when possible (Chen et al., 2016; Kugler et al., 2015; Lee et al, 2011).

5.2. Impact of forest type

The forest type is one of the factors expected to affect the accuracy of canopy height inversion from TDX coherence. This study observed that the performance of TDX height estimation was different for broadleaved and coniferous forests. The RMSE and R^2 revealed that, the accuracy for broadleaved forests were unstable across seasons, compared to coniferous forests. The average RMSEr (%) for broadleaved forests decreased from 29.9% of October acquisitions to 23.9% of January acquisitions. Whereas for coniferous forests the average RMSEr (%) remained stable for October (23.3%) and January acquisitions (21.0%). The same is true for the R^2. The average R^2 for October and January acquisitions were 0.13 and 0.46 (broadleaved) and 0.25 and 0.40 (coniferous forests), respectively. It can also be seen that the RMSE and R^2 of both forest types had a low difference for January acquisitions compared to October acquisitions. The difference in RMSE and R^2 between forest types in October acquisitions is mainly expected to be linked with leaf conditions. During leaf-on season, broadleaved forests have heterogenous canopy structure causing in loose of coherence, as compared to leaf-off season which are homogenous in their structure without leaves (Olesk et al., 2015a). In addition, in leaf-on condition of broadleaved forest, X-band has limited capability of penetration resulting in substantial estimation accuracy difference with coniferous forests, as compared to leaf-off season. In temperate forests, during leaf-off season, the penetration depth is high, and the volumetric information can be acquired, leading to better estimation accuracy (Erasmi et al., 2019; Kugler et al., 2014; Olesk et al., 2015b; Schlund et al., 2019). On the contrary, studies in boreal (Solberg et al., 2015) and tropical forests (Khati et al., 2917), stated that deep penetration of X-band during leaf-off season underestimates the height resulting in estimation error. However, it should be noted that the forest ecosystems are different which can not be compared to the current study. Moreover, Kugler et al. (2014) found different results for those forest ecosystems in relation to X band penetration and estimation error.

Another accuracy metrics (MAEr), which compared pixel by pixel, showed that for all acquisitions, the coniferous forests had significantly lower estimation error than broadleaved forests. While the significant variation in the October acquisitions is expected due to the leaf condition, the significant variation in January acquisitions showed that forest type could also influence estimation accuracy. This indicates that apart from leaf condition, there were other factors causing different estimation accuracy between the two forest types. One of the reasons could be the weather condition during the acquisitions. Both forest types may respond differently to the existed precipitation/temperature in relation to X-band backscatter. The presences of precipitation during and one day before the acquisition date might have affect both forest types differently. One indication for this could be that the January 19 acquisition had highest precipitation which also yielded highest MAEr difference between the two forest types. In addition, the difference in morphological characteristics of broadleaved and coniferous forests might contribute. Deciduous trees have strong ability of attenuating X-band waves than coniferous trees (Hoekman, 1987). X-band backscatter is assumed to be responsive to variations in leaf characteristics such as leaf area index, leaf moisture content and leaf curvature, trunk size, branch distribution and so on (McDonald et al., 1991). Given that coniferous and broadleaved forests have different morphological characteristics, the variation in height estimation accuracy of the two forest types is expected. Olesk et al. (2016) revealed that coniferous and broadleaved forests exhibited different X-band extinction properties, which possibly could be a source of variation for the estimation accuracy between the two forest types. In general, it is observed that coniferous forests are less affected by seasonal changes and unsuitable weather condition than broadleaved forests. In line with this study, Olesk et al. (2015b) and Schlund et al. (2019) also found that coniferous forests are least affected by seasonal variation and had better estimation accuracy than broadleaved forests. Hence, when canopy height estimation with the linear model is applied to broadleaved temperate forests, selecting acquisitions from leaf-off season and suitable weather conditions (cold and dry) is recommended.

5.3. Impact of slope and canopy cover

Slope is one of the factors that affects the TDX height estimation accuracy (Chen et al., 2018; Gomez et al., 2021; Kugler et al., 2015; Schlund et al., 2019). Especially slopes in the range direction alter the local incidence angle (Kugler et al., 2015). This modification of the incidence angle affects the coherence which may lead to biased height estimation (Kugler et al., 2015). In this study, the effect of slope on the estimation accuracy was mainly dependent on the HoA. The model had similar performance across slope classes for acquisition with HoA less than 45 m. Whereas for the acquisitions with high HoA the model did not work well in the steep slope. Contrary to this study, a study in temperate forest showed that estimation error was stable up to a slope of 20^0 (around 36%) regardless of the HoA (Schlund et al., 2019). However, this could depend on the composition of forest type, height class distribution and other factors across the slope classes. Nevertheless, Chen et al., 2018, recommended that for steep terrain, better estimation could be obtained when the ratio of HoA to canopy height ranged from 1 to 3. Similarly in this study, the two acquisitions where most of the pixels had the ratio of HoA to canopy height above 3, produced a significantly higher error in the steep slope class than the gentle and flat slope classes. Hence, to study the relationship of slope and TDX height estimation accuracy, appropriate selection of HoA with regard to the forest canopy height should be considered. In addition, impact of slopes should be further studied with stratification of forest type and under suitable weather conditions to reduce the complex interaction among different sources of errors.

Similar to the slope the impact of canopy cover was pronounced in acquisitions of January 19 and January 24 which have high HoA. The impact of canopy cover was not seen in the other three acquisitions which possibly is related to small HoA. The dense forests in the study area were mostly characterized with high canopy height which were poorly estimated with the small HoA. Appendix 8 showed that a linear increment of canopy height with increasing canopy cover percentage. Hence, for the study area with the given canopy height distribution across different canopy cover, it might be difficult to see impact of canopy cover when the HoA small. For the two acquisitions with high HoA, the MAEr showed substantial decrement as the canopy cover increases. Martone et al. (2012) explained for a dense canopy, high HoA are required to minimize the volume decorrelation effects. In fact, volume decorrelation is high in closed canopy as compared to open canopy which may lead to low coherence (Schlund et al., 2014, 2013) and then to high estimation error. When there is low canopy cover there is high possibility of microwaves interacting with the branches of trees which results in several direct returns, hence reduced decorrelation as compared to volume scattering of dense canopy from the leaves (Schlund et al., 2013). However, this is dependent on HoA and canopy height. The fact that January 19 and January 24 acquisition had high HoA (which improves the coherence), and the denser areas had high canopy height led to less estimation error in the high canopy cover areas. Note that these two acquisitions had better accuracy at the high canopy height levels (Appendix 7).

In general, the continuous values of slope and canopy cover were able to explain the variation in mean error with a very poor R^2 in broadleaved forest. In fact, these two factors could not strongly explain the variation in the coherence. They both contribute to 11% and 6% variations in coherence in broadleaved and coniferous forests, respectively. The coefficients indicated that the canopy cover had more impact than the slope. The reason that the impact of slope was not pronounced might be related to the fact that the study was limited to slope less than 20%, in which most of the slope lay in gentle slope. Studies suggested that the impact of slope is well visible when slope goes above 20^0 (around 36%) (Kugler et al., 2015; Leonardo et al., 2020; Schlund et al., 2019). In addition, the direction of the slopes in relation to the satellites were not accounted in this study which might have an impact in the relationship between slope and estimation accuracy. Kugler et al. (2015) elaborated that slope in range direction has higher impact than in the azimuth direction in modifying the incidence angle consequently affecting the coherence and estimation accuracy. Also, slopes facing towards and away from the satellite overestimate and underestimate the estimation, respectively (Kugler et al., 2015). One of the major limitations of the current study is treating all these slopes similarly. Also, the canopy gap volume was not investigated in this study. The combination of these limitations might have induced some influences when attempting to examine the contribution of slope and canopy cover in explaining the variation in the estimation error. Other factors like forest composition, vertical and horizontal structure, vegetation water content, temperature and other vegetation morphological characteristics which were not accounted in this study are expected to influence the coherence and consequently the estimation error (Demirpolat, 2012; Erasmi et al., 2019).

6. CONCLUSIONS

The result of this study suggested that single polarized TDX coherence can estimate a canopy height with reasonable accuracy of less than 6 m using linear model. With small HoA, sinc model also exhibited similar accuracy, despite its overestimation when using high HoA (RMSE>12 m). Season of acquisition and HoA influenced the canopy height estimation from TDX coherence. In general, it has been observed that acquisitions with high HoA yielded better accuracies. However, each acquisition produced different accuracies across different canopy heights. Additionally, the season of acquisition, which can be explained in terms of leaf and weather condition influenced the estimation accuracy. The accuracy in broadleaved forest was affected by season change, compared to coniferous forests. When it is leaf-on season, and the temperature and precipitation is low, the accuracy differences between the two forest types tended to be low. The study observed that similar weather conditions (wet and hot weather) affect the estimation accuracy of both forest types differently.

Furthermore, slope and canopy cover had influenced the estimation accuracy, but this was limited only to the acquisitions with high HoA. The impact of slope was minimal as compared to the impact of canopy cover. This can be due to the study area was dominated by gentle slope class; hence, it might not be a suitable area to show the impact of slope. The combination of slope and canopy cover poorly explained the variation in absolute estimation error for both forest types. This apparently indicated that, there are other factors, not accounted in this study, that determine the absolute estimation error. This could be an interesting research topic for future studies.

In general, TDX is a good option in temperate forests to estimate canopy height, thereby biomass, when it is required to cover large area and frequent measurement. However, attentions should be given to acquisition parameters, like HoA, climatic variables such as temperature and precipitation, and characteristics of the target scatterer (forest) such as canopy cover, canopy height and slope. More importantly, an interaction between the aforementioned variables should get a special attention. Especially, broadleaved forests required careful selection of acquisitions in relation to leaf and weather conditions so as to acquire moderate accuracy. In spite of the limitations, this study investigated that single polarized TDX coherence data can give encouraging accuracies without using external data which is very useful for large area mapping and biomass quantification. Future studies should focus on examining factors affecting the estimation error in forested areas at pixel level when estimating TDX canopy height using linear/sinc models.

LIST OF REFERENCES

Abdullahi, S., Kugler, F., Pretzsch, H., 2016. Prediction of stem volume in complex temperate forest stands using TanDEM-X SAR data. Remote Sensing of Environment 174, 197–211. https://doi.org/10.1016/J.RSE.2015.12.012

Aulinger, T., Mette, T., Papathanassiou, K.P., Hajnsek, I., Heurich, M., Krzystek, P., 2005. Validation of heights from interferometric sar and lidar over the temperate forest site "nationalpark bayerischer wald." In ESA Special Publication 586, 11. https://adsabs.harvard.edu/pdf/2005ESASP.586...11A

Bamler, R., Hartl, P., 1998. Synthetic aperture radar interferometry. Inverse Problems 14, R1. https://doi.org/10.1088/0266-5611/14/4/001

Canadell, J.G., Raupach, M.R., 2008. Managing forests for climate change mitigation. Science (New York, N.Y.) 320, 1456–1457. https://doi.org/10.1126/SCIENCE.1155458

Chave, J., Réjou-Méchain, M., Búrquez, A., Chidumayo, E., Colgan, M.S., Delitti, W.B.C., Duque, A., Eid, T., Fearnside, P.M., Goodman, R.C., Henry, M., Martínez-Yrízar, A., Mugasha, W.A., Muller-Landau, H.C., Mencuccini, M., Nelson, B.W., Ngomanda, A., Nogueira, E.M., Ortiz-Malavassi, E., Pélissier, R., Ploton, P., Ryan, C.M., Saldarriaga, J.G., Vieilledent, G., 2014. Improved allometric models to estimate the aboveground biomass of tropical trees. Global Change Biology 20, 3177–3190. https://doi.org/10.1111/GCB.12629

Chen, H., Beaudoin, A., Hill, D.A., Cloude, S.R., Skakun, R.S., Marchand, M., 2019. Mapping Forest Height from TanDEM-X Interferometric Coherence Data in Northwest Territories, Canada. Canadian Journal of Remote Sensing 45, 290–307. https://doi.org/10.1080/07038992.2019.1604119

Chen, H., Cloude, S.R., Goodenough, D.G., 2016. Forest Canopy Height Estimation Using Tandem-X Coherence Data. IEEE Journal of Selected Topics in Applied Earth Observations and Remote Sensing 9, 3177–3188. https://doi.org/10.1109/JSTARS.2016.2582722

Chen, H., Cloude, S.R., Goodenough, D.G., Hill, D.A., Nesdoly, A., 2018. Radar forest height estimation in mountainous terrain using Tandem-X coherence data. IEEE Journal of Selected Topics in Applied Earth Observations and Remote Sensing 11, 3443–3452. https://doi.org/10.1109/JSTARS.2018.2866059

Chen, H., Cloude, S.R., White, J.C., 2021. Using GEDI Waveforms for Improved TanDEM-X Forest Height Mapping: A Combined SINC + Legendre Approach. Remote Sensing 2021, Vol. 13, Page 2882 13, 2882. https://doi.org/10.3390/RS13152882

Chen, H., Goodenough, D.G., Cloude, S.R., Padda, P., 2015. Wide area forest height mapping using Tandem-X standard mode data. International Geoscience and Remote Sensing Symposium (IGARSS) 2015-November, 3782–3785. https://doi.org/10.1109/IGARSS.2015.7326647

Cloude, S.R., 1998. Polarimetric sar interferometry. IEEE Transactions on Geoscience and Remote Sensing 36, 1551–1565. https://doi.org/10.1109/36.718859

Cloude, S.R., Pettier, E., 1996. A review of target decomposition theorems in radar polarimetry. IEEE Transactions on Geoscience and Remote Sensing 34, 498–518. https://doi.org/10.1109/36.485127

Coops, N.C., Hilker, T., Wulder, M.A., St-Onge, B., Newnham, G., Siggins, A., Trofymow, J.A., 2007. Estimating canopy structure of Douglas-fir forest stands from discrete-return LiDAR. Trees - Structure and Function 21, 295–310. https://doi.org/10.1007/s00468-006-0119-6

DeFries, R., Achard, F., Brown, S., Herold, M., Murdiyarso, D., Schlamadinger, B., de Souza, C., 2007. Earth observations for estimating greenhouse gas emissions from deforestation in developing countries. Environmental Science and Policy 10, 385–394. https://doi.org/10.1016/j.envsci.2007.01.010

Demirpolat, C., 2012. X-band Interferometric Radar for Mapping Temporal Variability in Forest (Master's Thesis). Aalto University, Espoo.

Douillard, B., Underwood, J., Kuntz, N., Vlaskine, V., Quadros, A., Morton, P., Frenkel, A., 2011. On the segmentation of 3D lidar point clouds. Proceedings - IEEE International Conference on Robotics and Automation 2798–2805. https://doi.org/10.1109/ICRA.2011.5979818

Erasmi, S., Semmler, M., Schall, P., Schlund, M., 2019. Sensitivity of Bistatic TanDEM-X Data to Stand Structural Parameters in Temperate Forests. Remote Sensing 2019, Vol. 11, Page 2966 11, 2966. https://doi.org/10.3390/RS11242966

European Environment Agency, 2021. European Union, Copernicus Land Monitoring Service. [WWW Document]. URL https://land.copernicus.eu/ (accessed 12.9.21).

FAO. 2020. Global Forest Resources Assessment 2020: Main report. Rome. https://doi.org/10.4060/ca9825en

Ferraz, A., Saatchi, S., Mallet, C., Meyer, V., 2016. Lidar detection of individual tree size in tropical forests. Remote Sensing of Environment 183, 318–333. https://doi.org/10.1016/J.RSE.2016.05.028

Fu, H., Wang, C., Zhu, J., Xie, Q., Zhang, B., 2016. Estimation of Pine Forest Height and Underlying DEM Using Multi-Baseline P-Band PolInSAR Data. Remote Sensing 2016, Vol. 8, Page 820 8, 820. https://doi.org/10.3390/RS8100820

Gibbs, H.K., Brown, S., Niles, J.O., Foley, J.A., 2007. Monitoring and estimating tropical forest carbon stocks: making REDD a reality. Environ. Res. Lett 2, 13. https://doi.org/10.1088/1748-9326/2/4/045023

Gomez, C., Lopez-Sanchez, J.M., Romero-Puig, N., Zhu, J., Fu, H., He, W., Xie, Y., Xie, Q., 2021. Canopy Height Estimation in Mediterranean Forests of Spain with TanDEM-X Data. IEEE Journal of Selected Topics in Applied Earth Observations and Remote Sensing 14, 2956–2970. https://doi.org/10.1109/JSTARS.2021.3060691

Guliaev, R., Cazcarra-Bes, V., Pardini, M., Papathanassiou, K., 2021. Forest Height Estimation by Means of TanDEM-X InSAR and Waveform Lidar Data. IEEE Journal of Selected Topics in Applied Earth Observations and Remote Sensing 14, 3084–3094. https://doi.org/10.1109/JSTARS.2021.3058837

Hajnsek, I., Kugler, F., Lee, S.K., Papathanassiou, K.P., 2009. Tropical-forest-parameter estimation by means of Pol-InSAR: The INDREX-II campaign. IEEE Transactions on Geoscience and Remote Sensing 47, 481–493. https://doi.org/10.1109/TGRS.2008.2009437

Hein, L., 2011. Economic Benefits Generated by Protected Areas: The Case of the Hoge Veluwe Forest, the Netherlands. Ecology and Society 16. https://www.jstor.org/stable/26268887

Henderson, F.M., Lewis, A.J., American Society for Photogrammetry and Remote Sensing., 1998. Principles and applications of imaging radar. J. Wiley, New York.

Hoberg, G., Peterson St-Laurent, G., Schittecatte, G., Dymond, C.C., 2016. Forest carbon mitigation policy: A policy gap analysis for British Columbia. Forest Policy and Economics 69, 73–82. https://doi.org/10.1016/J.FORPOL.2016.05.005

Hoekman, D.H., 1987. Measurements of the backscatter and attenuation properties of forest stands at X-, C- and L-band. Remote Sensing of Environment 23, 397–416. https://doi.org/10.1016/0034-4257(87)90098-8

Home Page - GEDI [WWW Document], n.d. URL https://gedi.umd.edu/ (accessed 12.6.21).

Iaaich, H., Moussadek, R., Baghdad, B., Mrabet, R., Douaik, A., Abdelkrim, D., Bouabdli, A., 2016. Soil erodibility mapping using three approaches in the Tangiers province –Northern Morocco. International Soil and Water Conservation Research 4, 159–167. https://doi.org/10.1016/J.ISWCR.2016.07.001

Kachamba, D.J., Ørka, H.O., Gobakken, T., Eid, T., Mwase, W., 2016. Biomass estimation using 3D data from unmanned aerial vehicle imagery in a tropical woodland. Remote Sensing 8, 968. https://doi.org/10.3390/rs8110968

Khati, U., Singh, G., Ferro-Famil, L., 2017. Analysis of seasonal effects on forest parameter estimation of Indian deciduous forest using TerraSAR-X PolInSAR acquisitions. Remote Sensing of Environment 199, 265–276. https://doi.org/10.1016/J.RSE.2017.07.019

KNMI - Daily values precipitation stations [WWW Document], n.d. URL https://www.knmi.nl/nederland-nu/klimatologie/monv/reeksen#Z (accessed 12.9.21).

Krieger, G., Hajnsek, I., Papathanassiou, K.P., Younis, M., Moreira, A., 2010. Interferometric Synthetic Aperture Radar (SAR) Missions Employing Formation Flying. Proceedings of the IEEE 5, 816–843. https://doi.org/10.1109/JPROC.2009.2038948

Kugler, F., Lee, S.K., Hajnsek, I., Papathanassiou, K.P., 2015. Forest Height Estimation by Means of Pol-InSAR Data Inversion: The Role of the Vertical Wavenumber. IEEE Transactions on Geoscience and Remote Sensing 53, 5294–5311. https://doi.org/10.1109/TGRS.2015.2420996

Kugler, F., Schulze, D., Hajnsek, I., Pretzsch, H., Papathanassiou, K.P., 2014. TanDEM-X Pol-InSAR performance for forest height estimation. IEEE Transactions on Geoscience and Remote Sensing 52, 6404–6422. https://doi.org/10.1109/TGRS.2013.2296533

Kuiters, A.T., T A Groot Bruinderink, G.W., LAMMERTSMA Kuiters A T, D.R., Bruinderink W T A, G.G., R, L.D., 2005a. Facilitative and competitive interactions between sympatric cattle, red deer and wild boar in Dutch woodland pastures. Acta Theriologica 2004 50:2 50, 241–252. https://doi.org/10.1007/BF03194487

Kuiters, A.T., van der Sluijs, L.A.M., Wytema, G.A., 2005b. Selective bark-stripping of beech, Fagus sylvatica, by free-ranging horses. Acta Theriologica 50, 241–252. https://doi.org/10.1016/j.foreco.2005.09.019

Kwaliteitsbeschrijving | AHN [WWW Document], n.d. URL https://www.ahn.nl/kwaliteitsbeschrijving (accessed 10.28.21).

Lee, S., Kugler, F., Papathanassiou, K., Hajnsek, I., 2011. Multibaseline polarimetric SAR interferometry forest height inversion approaches. In Proceedings of ESA POLinSAR Workshop. https://elib.dlr.de/74010/1/P2133503Lee.pdf

Leonardo, E.M.C., Watt, M.S., Pearse, G.D., Dash, J.P., Persson, H.J., 2020. Comparison of TanDEM-X InSAR data and high-density ALS for the prediction of forest inventory attributes in plantation forests with steep terrain. Remote Sensing of Environment 246, 111833. https://doi.org/10.1016/J.RSE.2020.111833

Liski, J., Korotkov, A. v., Prins, C.F.L., Karjalainen, T., Victor, D.G., Kauppi, P.E., 2003. Increased Carbon Sink in Temperate and Boreal Forests. Climatic Change 2003 61:1 61, 89–99. https://doi.org/10.1023/A:1026365005696

Lovell, J.L., Jupp, D.L.B., Culvenor, D.S., Coops, N.C., 2003. Using airborne and ground-based ranging lidar to measure canopy structure in Australian forests. Canadian Journal of Remote Sensing 29, 607–622. https://doi.org/10.5589/M03-026

Lu, D., Chen, Q., Wang, G., Liu, L., Li, G., Moran, E., 2016. A survey of remote sensing-based aboveground biomass estimation methods in forest ecosystems. International Journal of Digital Earth 9, 63–105. https://doi.org/10.1080/17538947.2014.990526

Martone, M., Bräutigam, B., Rizzoli, P., Gonzalez, C., Bachmann, M., Krieger, G., 2012. Coherence evaluation of TanDEM-X interferometric data. ISPRS Journal of Photogrammetry and Remote Sensing 73, 21–29. https://doi.org/10.1016/J.ISPRSJPRS.2012.06.006

McDonald, K.C., Dobson, M.C., Ulaby, F.T., 1991. Modeling multi-frequency diurnal backscatter from a walnut orchard. IEEE Transactions on Geoscience and Remote Sensing 29, 852–863. https://doi.org/10.1109/TGRS.1991.1019469

McElhinny, C., Gibbons, P., Brack, C., Bauhus, J., 2005. Forest and woodland stand structural complexity: Its definition and measurement. Forest Ecology and Management 218, 1–24. https://doi.org/10.1016/J.FORECO.2005.08.034

Miuigan, G.W., Cooper, Martha C, Milligan, Glenn W, Milligan, G W, Cooper, M C, 1988. A study of standardization of variables in cluster analysis. Journal of Classification 1988 5:2 5, 181–204. https://doi.org/10.1007/BF01897163

Ni, W., Zhang, Z., Sun, G., Guo, Z., He, Y., 2014. The Penetration Depth Derived from the Synthesis of ALOS/PALSAR InSAR Data and ASTER GDEM for the Mapping of Forest Biomass. Remote Sensing 2014, Vol. 6, Pages 7303-7319 6, 7303–7319. https://doi.org/10.3390/RS6087303

Olesk, A., Praks, J., Antropov, O., Zalite, K., Arumäe, T., Voormansik, K., 2016. Interferometric SAR Coherence Models for Characterization of Hemiboreal Forests Using TanDEM-X Data. Remote Sensing 2016, Vol. 8, Page 700 8, 700. https://doi.org/10.3390/RS8090700

Olesk, A., Voormansik, K., Tamm, T., Noorma, M., Praks, J., 2015a. Seasonal effects on the estimation of height of boreal and deciduous forests from interferometric TanDEM-X coherence data. In Earth Resources and Environmental Remote Sensing/GIS Applications VI (Vol. 9644, pp. 22-29). https://doi.org/10.1117/12.2194340

Olesk, A., Voormansik, K., Vain, A., Noorma, M., Praks, J., 2015b. Seasonal Differences in Forest Height Estimation from Interferometric TanDEM-X Coherence Data. IEEE Journal of Selected Topics in Applied Earth Observations and Remote Sensing 8, 5565–5572. https://doi.org/10.1109/JSTARS.2015.2501648

Persson, H.J., Fransson, J.E.S., 2016. Comparison between TanDEM-X- and ALS-based estimation of aboveground biomass and tree height in boreal forests. Scandinavian Journal of Forest Research 32, 306–319. https://doi.org/10.1080/02827581.2016.1220618

Persson, H.J., Olsson, H., Soja, M.J., Ulander, L.M.H., Fransson, J.E.S., 2017. Experiences from Large-Scale Forest Mapping of Sweden Using TanDEM-X Data. Remote Sensing 2017, Vol. 9, Page 1253 9, 1253. https://doi.org/10.3390/RS9121253

Pirotti, F., 2011. Analysis of full-waveform LiDAR data for forestry applications: a review of investigations and methods. iForest - Biogeosciences and Forestry 4, 100. https://doi.org/10.3832/IFOR0562-004

Popescu, S.C., Wynne, R.H., 2004. Seeing the Trees in the Forest: Using Lidar and Multispectral Data Fusion with Local Filtering and Variable Window Size for Estimating Tree Height. undefined 70, 589–604. https://doi.org/10.14358/PERS.70.5.589

Qi, W., Dubayah, R.O., 2017. Forest structure modeling of a coniferous forest using TanDEM-X InSAR and simulated GEDI lidar data. undefined 2017-July, 914–917. https://doi.org/10.1109/IGARSS.2017.8127101

Qi, W., Lee, S.K., Hancock, S., Luthcke, S., Tang, H., Armston, J., Dubayah, R., 2019. Improved forest height estimation by fusion of simulated GEDI Lidar data and TanDEM-X InSAR data. Remote Sensing of Environment 221, 621–634. https://doi.org/10.1016/J.RSE.2018.11.035

Richards, J.A., 2009. Remote sensing with imaging radar (Vol. 1). Berlin/Heidelberg, Germany: Springer.

Sadeghi, St-Onge, B., Leblon, B., Simard, M., 2016. Canopy Height Model (CHM) Derived from a TanDEM-X InSAR DSM and an Airborne Lidar DTM in Boreal Forest. IEEE Journal of Selected Topics in Applied Earth Observations and Remote Sensing 9, 381–397. https://doi.org/10.1109/JSTARS.2015.2512230

Sadeghi, Y., St-Onge, B., Leblon, B., Simard, M., Papathanassiou, K., 2014. Mapping forest canopy height using TanDEM-X DSM and airborne LiDAR DTM. International Geoscience and Remote Sensing Symposium (IGARSS) 76–79. https://doi.org/10.1109/IGARSS.2014.6946359

Sadeghi, Y., St-Onge, B., Leblon, B., Simard, M., 2017. Effects of TanDEM-X Acquisition Parameters on the Accuracy of Digital Surface Models of a Boreal Forest Canopy. Canadian Journal of Remote Sensing 43, 194–207. https://doi.org/10.1080/07038992.2017.1291336

Schimel, D.S., House, J.I., Hibbard, K.A., Bousquet, P., Ciais, P., Peylin, P., Braswell, B.H., Apps, M.J., Baker, D., Bondeau, A., Canadell, J., Churkina, G., Cramer, W., Denning, A.S., Field, C.B., Friedlingstein, P., Goodale, C., Heimann, M., Houghton, R.A., Melillo, J.M., Moore, B., Murdiyarso, D., Noble, I., Pacala, S.W., Prentice, I.C., Raupach, M.R., Rayner, P.J., Scholes, R.J., Steffen, W.L., Wirth, C., 2001. Recent patterns and mechanisms of carbon exchange by terrestrial ecosystems. Nature 414, 169–172. https://doi.org/10.1038/35102500

Schlund, M., Magdon, P., Eaton, B., Aumann, C., Erasmi, S., 2019. Canopy height estimation with TanDEM-X in temperate and boreal forests. International Journal of Applied Earth Observation and Geoinformation 82, 101904. https://doi.org/10.1016/j.jag.2019.101904

Schlund, M., Poncet, F. von, Kuntz, S., Hoekman, D.H., 2013. Relationship of canopy cover with TanDEM-X features in a tropical peat swamp forest. GI_Forum 2013, Volume 1. Verlag der Österreichischen Akademie der Wissenschaften, pp. 109–112. https://doi.org/10.1553/GISCIENCE2013S109

Schlund, M., von Poncet, F., Hoekman, D.H., Kuntz, S., Schmullius, C., 2014. Importance of bistatic SAR features from TanDEM-X for forest mapping and monitoring. Remote Sensing of Environment 151, 16–26. https://doi.org/10.1016/J.RSE.2013.08.024

Sedjo, R.A., Toman, M., 2001. Can Carbon Sinks Be Operational? RFF Workshop Proceedings. https://doi.org/10.22004/AG.ECON.10480

Solberg, S., Weydahl, D.J., Astrup, R., 2015. Temporal stability of X-band single-pass InSAR heights in a spruce forest: Effects of acquisition properties and season. IEEE Transactions on Geoscience and Remote Sensing 53, 1607–1614. https://doi.org/10.1109/TGRS.2014.2346473

Te Linde, B., van den Berg, L.J., van Rosmalen, R., (2012) Kartering Flora en Vegetatie Nationaal Park Veluwezoom [Mapping Flora and Vegetation National Park Veluwezoom]. Stichting Berglinde, in opdracht van Natuurmonumenten Gelderland [Berglinde Foundation, commissioned by Natural Monuments Gelderland].

Xie, Q., Zhu, J., Wang, C., Fu, H., Lopez-Sanchez, J.M., Ballester-Berman, J.D., 2017. A Modified Dual-Baseline PolInSAR Method for Forest Height Estimation. Remote Sensing 2017, Vol. 9, Page 819 9, 819. https://doi.org/10.3390/RS9080819

Zhang, Z., Cao, L., She, G., 2017. Estimating Forest Structural Parameters Using Canopy Metrics Derived from Airborne LiDAR Data in Subtropical Forests. Remote Sensing 2017, Vol. 9, Page 940 9, 940. https://doi.org/10.3390/RS9090940

Zink, M., Bachmann, M., Bräutigam, B., Fritz, T., Hajnsek, I., Krieger, G., Moreira, A., Wessel, B., 2014. TanDEM-X: The new global DEM takes shape. IEEE Geoscience and Remote Sensing Magazine 2, 8–23. https://doi.org/10.1109/MGRS.2014.2318895

APPENDICES

Appendix 1. Absolute error map of different acquisitions

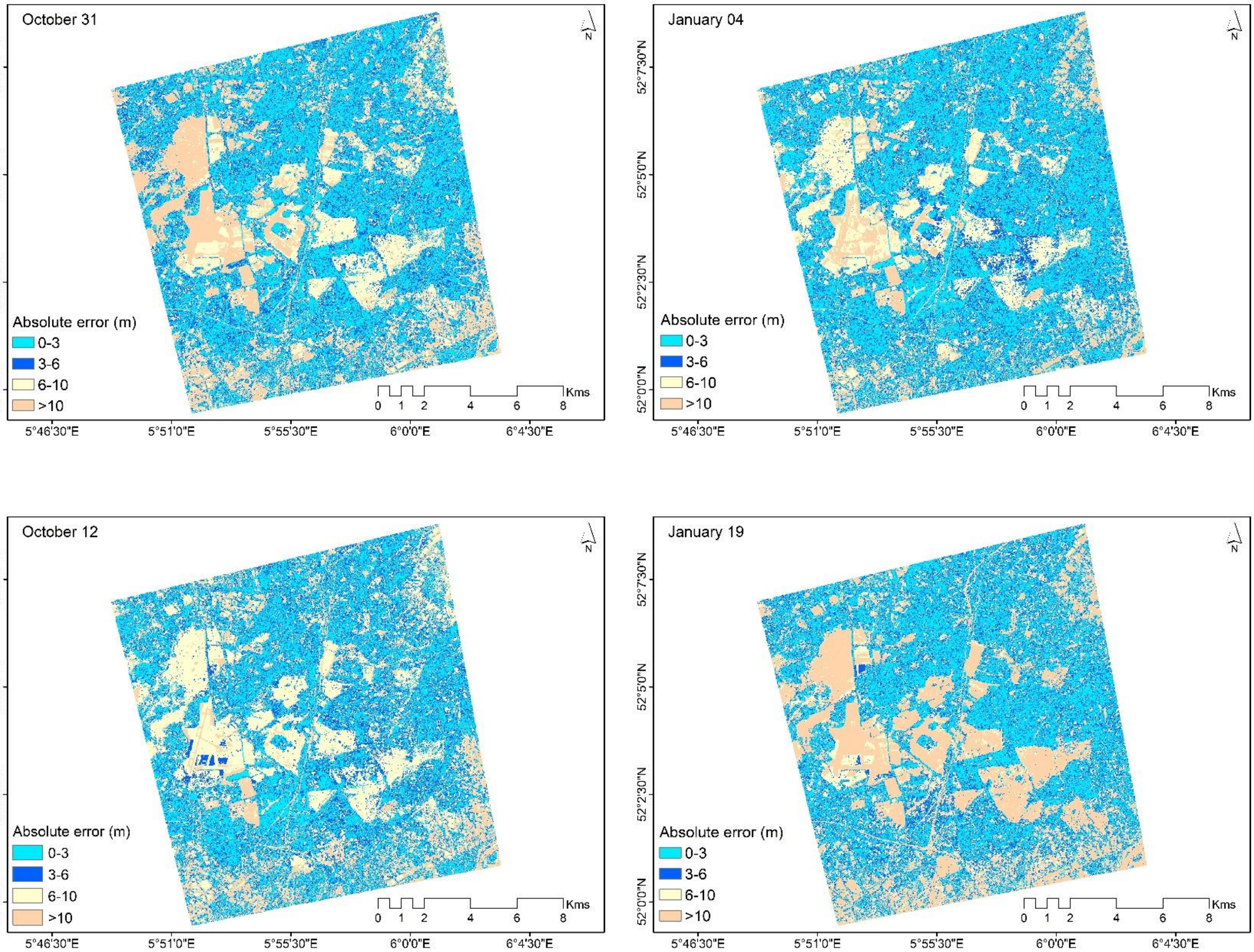

Appendix 2. Comparison of CHM and TDX estimated height for linear models of different acquisitions

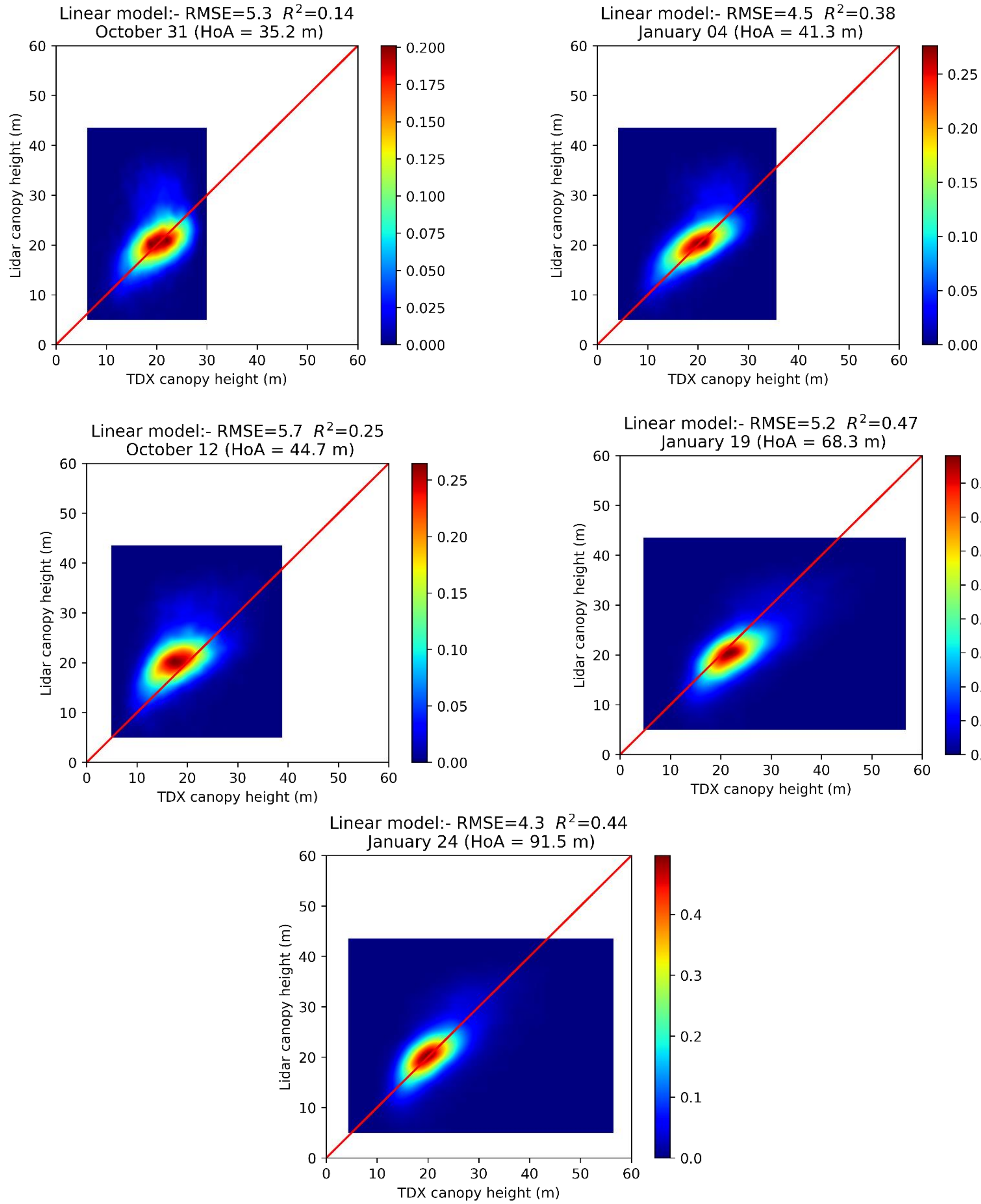

Appendix 3. Comparison of CHM and TDX estimated height for sinc models of different acquisitions

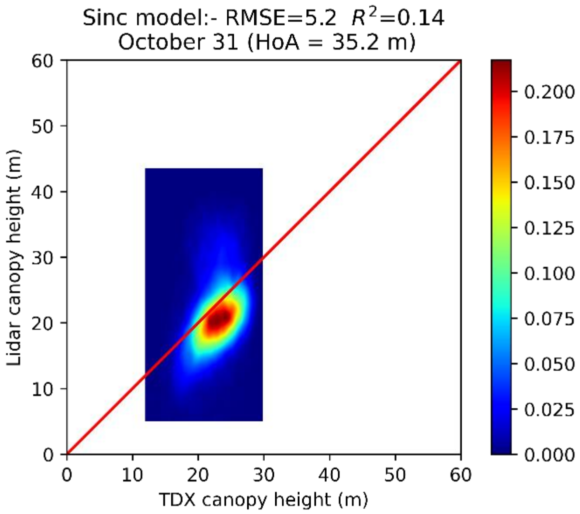

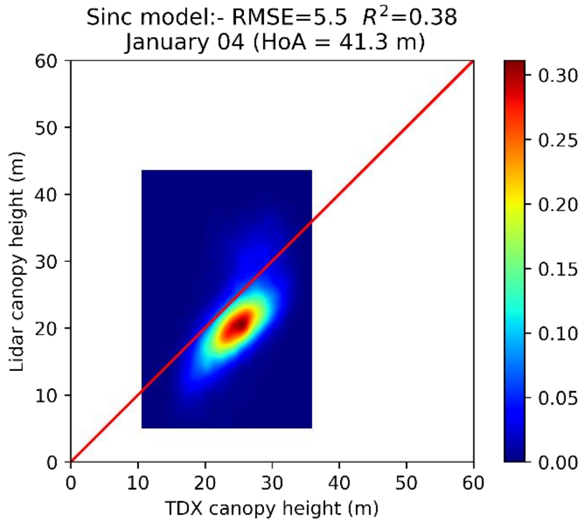

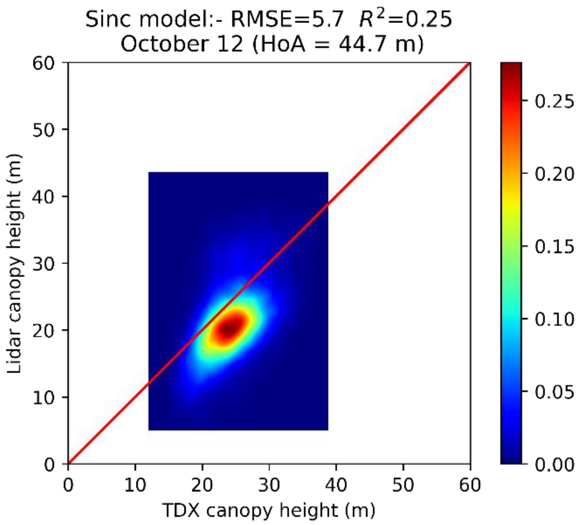

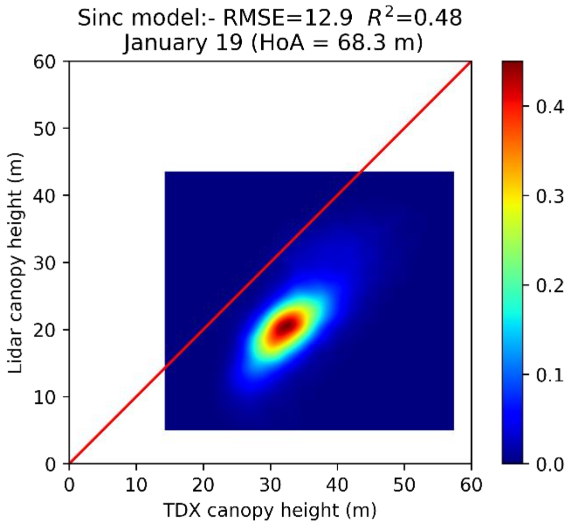

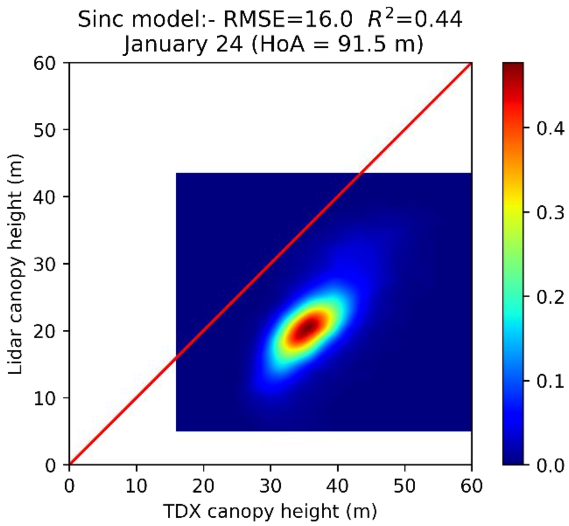

Appendix 4. Comparison of CHM and TDX estimated height (Linear) of different acquisitions in broadleaved forests

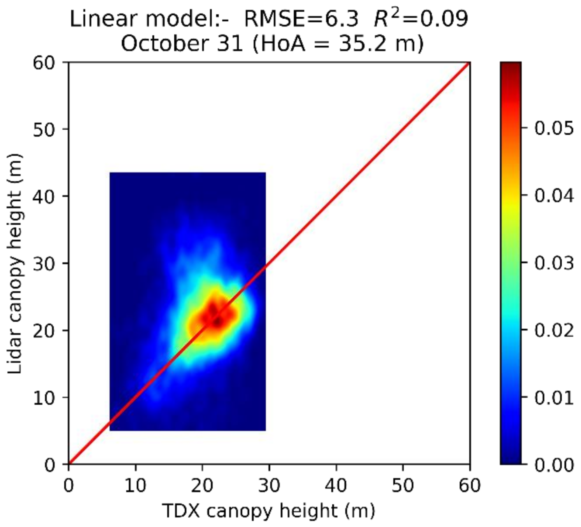

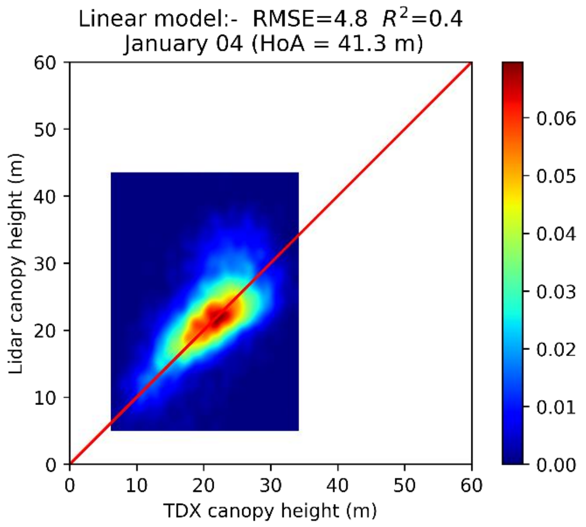

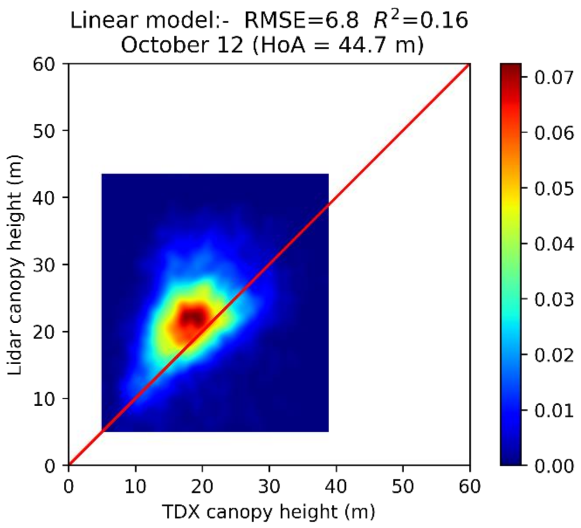

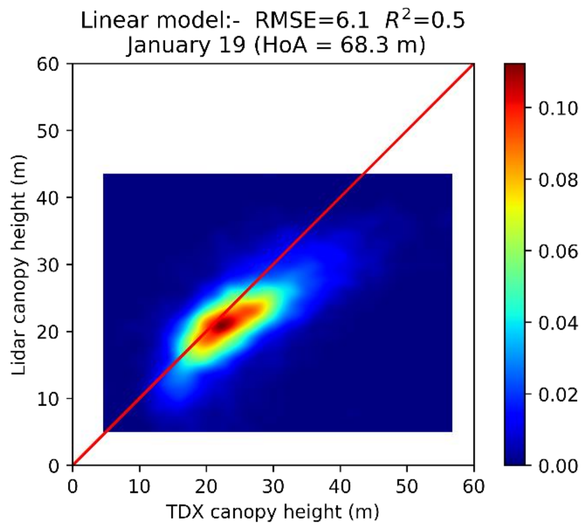

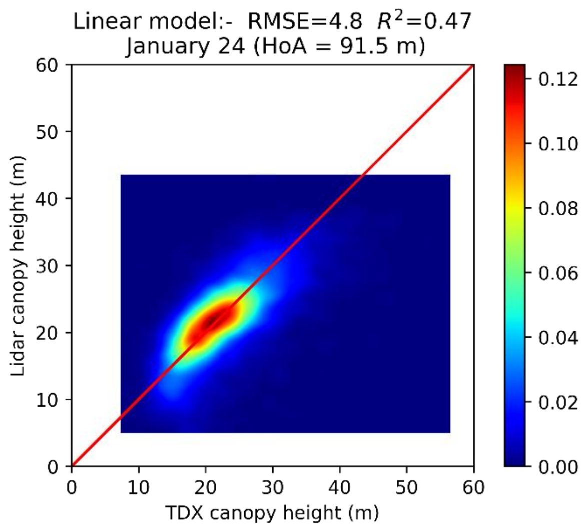

Appendix 5. Comparison of CHM and TDX estimated height (Linear) of different acquisitions in coniferous forests

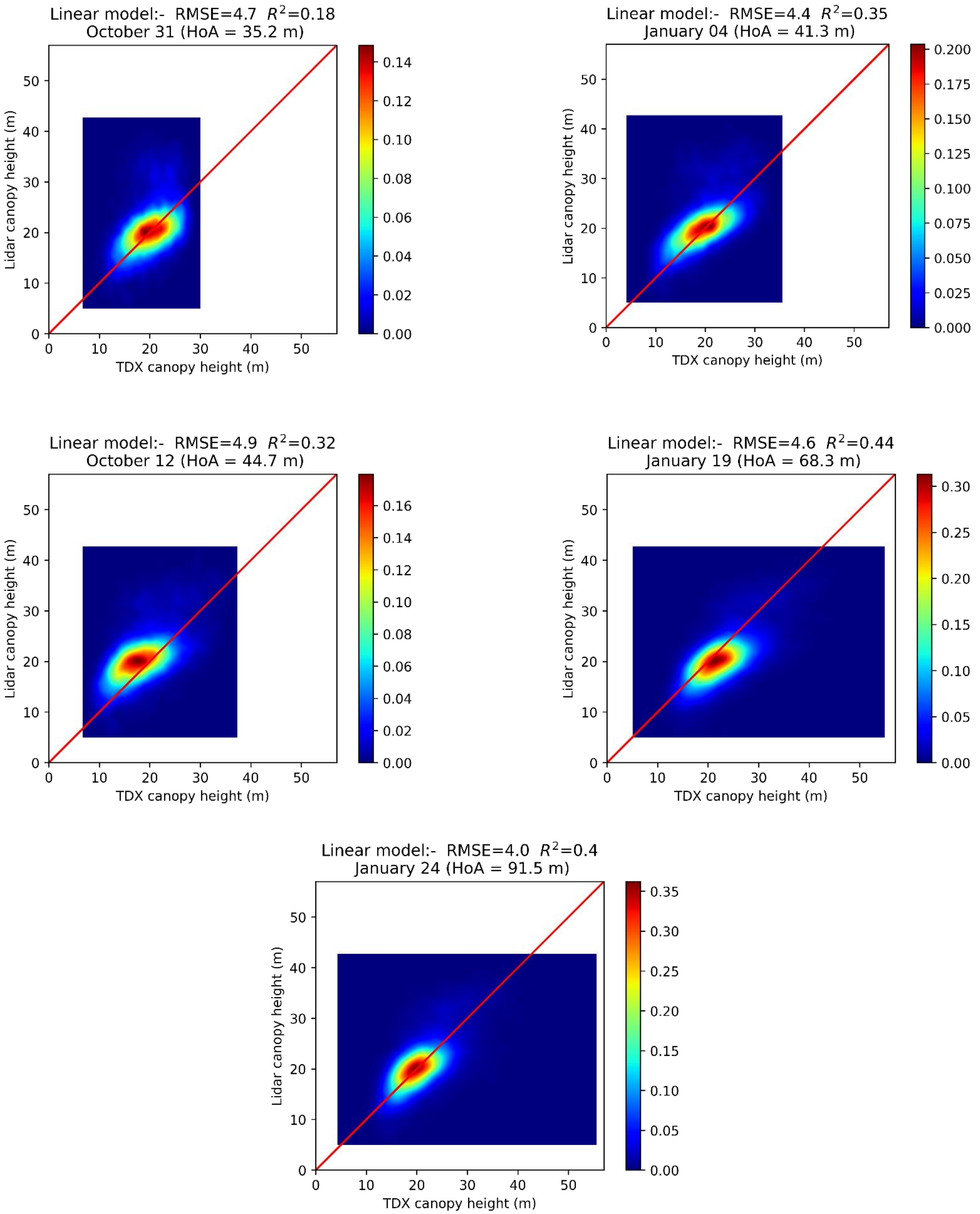

Appendix 6. Canopy cover percentage of the study area

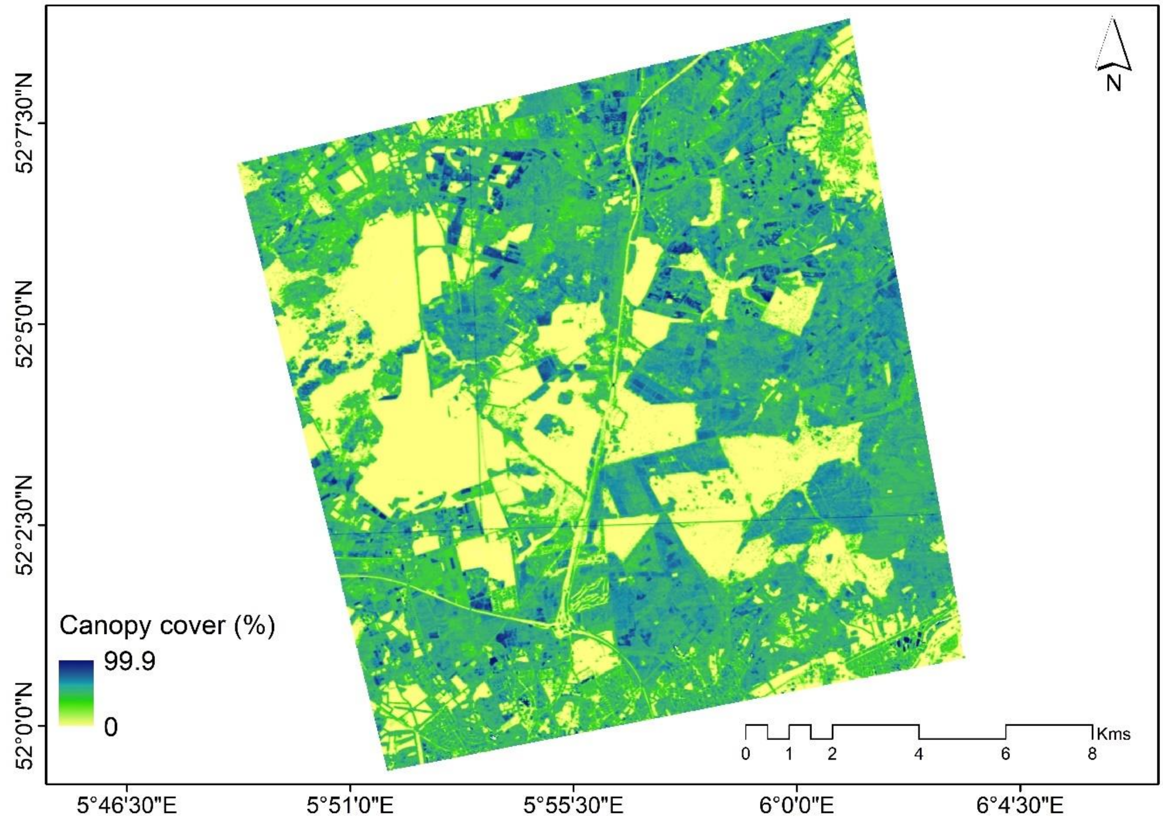

Appendix 7. Color scaled table showing RMSE (m) across different canopy height classes for all acquisitions (The value increase from green to red)

			Height class (m)					
	Acq. id	HoA	5 to 10	10 to 15	15 to 20	20 to 25	25 to 30	>30
RMSE (m)	October 31	35.2	8.3	4.5	3.5	3.4	6.7	13.1
	January 4	41.3	6.3	3.3	3.3	3.6	5.3	10.2
	October 12	44.7	7.8	3.8	3.9	4.8	7.6	11.8
	January 19	68.3	10.6	5.8	4.5	4.6	6.2	6.9
	January 24	91.5	9.9	5	3.6	3.6	5	6.8

Appendix 8. Color scaled table showing relationships between grouped canopy cover and MAEr for all acquisitions (The value increase from green to red)

		MAEr (%)				
Canopy cover (%)	Mean canopy height (m)	October 31	January 04	October 12	January 19	January 24
0 to 5	15.4	41.3	31.4	39.1	54.8	61.3
5 to 10	15.9	32.8	25.7	32.1	42	45.2
10 to 15	16.6	31.6	24.5	26.7	37.7	36.7
15 to 20	17.2	27.3	22.6	26.7	33.7	32.8
20 to 25	17.7	25	19.3	22.9	29.4	24.8
25 to 30	18.5	22.2	18.4	21.5	25.4	20.5
30 to 35	19.7	18.6	15.3	18.4	20.9	17.1
35 to 40	20.3	17	14.7	17.9	20.3	15.8
40 to 45	21.1	16.6	14.2	18.1	19.8	14.3
45 to 50	22.1	16.7	13.9	19.2	19.3	13.5
50 to 55	22.4	17.3	14.1	20	18.5	13.5
55 to 60	21.5	16.4	14.7	20.1	17.3	13.8
60 to 65	20.8	17	15.8	20.9	17.2	13.5
65 to 70	21.1	18.2	19.3	22.2	17.8	14.8
70 to 75	23.1	21.8	24.8	24.8	16.8	16.7
75 to 80	26.8	27.7	28.3	25.2	15.9	18.7
80 to 85	27.8	29.6	30.4	26.9	14.9	19.4
85 to 100	27.9	30.8	34	31.6	17	21.5